Recombinant CCL17 Shifts Microglial Phenotype and Protects Neurons from Oxygen-Glucose Deprivation/Reoxygenation (OGD/R) Injury

Inauguraldissertation

zur Erlangung des Grades eines Doktors der Medizin

des Fachbereichs Medizin

der Justus-Liebig-Universität Gießen

vorgelegt von Luan Tengfei

aus Qingdao, China

Gießen (2025)

Aus dem Fachbereich Medizin der Justus-Liebig-Universität Gießen

Universitätsklinikum Gießen und Marburg, Standort Gießen

Medizinisches Zentrum für Neurologie

Neurologische Klinik

Experimentelle Neurologie

Gutachter: Prof. Dr. med. Thorsten R. Döppner

Gutachter: Prof. Dr. Andreas Meinhardt

Tag der Disputation: 13.07.2026

INHALTSVERZEICHNIS

Seite

1. INTRODUCTION

1.1. Stroke

Stroke is recognized for its sudden breakdown in the brain's blood supply due to vessel rupture or blockage causing insufficient perfusion and subsequent injury to brain tissue (Donnan et al. 2008). Stroke is a major global health issue that causes high mortality and disability rates, as per data from The Lancet Neurology in March 2019 based on the year 2016 stats. Comparing to previous data, the number of deaths caused by stroke sharply declined between 1990 and 2016, but there was hardly any change in the rate of onset, meaning that the probability of occurrence is still large (Collaborators 2019).

1.2. Ischemic stroke

Clinically, most strokes are ischemic, and the remaining hemorrhagic proportion is less than 20%. Ischemic stroke is due to the sudden or gradually progressing occlusion of key cerebral vessels in the brain, causing a severe interruption of blood supply to specific regions and ultimately resulting in neuronal death or permanent neurological deficits (Garcia 1984; Hinkle and Guanci 2007; Whiteley et al. 2009). In the infarct core, blood flow usually decreases to 10%–25% of normal levels, leading to swift and permanent injury to neurons. The peri-infarct region, which borders the core, is called ischemic penumbra and this is an area without sufficient perfusion but it’s not completely infarcted (van der Worp and van Gijn 2007; Lo 2008). In the penumbra region, cells can survive for hours. If this region is soon restored to blood supply, the spread of injury can be prevented and cell viability maintained. Therefore, the purpose of early reperfusion is to restore blood flow to the penumbra and to prevent further infarction.

In ischemic stroke, the main sources of thrombotic and embolic material that can block cerebral arteries are typically atherosclerotic plaques in large arteries or cardiovascular conditions such as atrial arrhythmias. Small vessel disease, caused by conditions like high cholesterol or diabetes, can also contribute to brain injury (Sacco 1997). Understanding stroke causes is crucial for effective treatment and prevention. In addition to controlling

the risk factors to prevent stroke, appropriate therapeutic interventions during the acute and recovery phases are essential to reducing mortality, disability, and the recurrence of ischemic events.

At present, there are only two types of effective clinical treatment for ischemic stroke: intravenous thrombolysis and intra-arterial mechanical thrombectomy. Alteplase, a recombinant tissue plasminogen activator (tPA), is commonly used as a thrombolytic agent (National Institute of Neurological and Stroke rt 1995). Clinical trials have shown that intravenous thrombolysis with alteplase within 4.5 hours of ischemic stroke onset can improve neurological function recovery at 3-6 months in eligible patients. However, intravenous thrombolysis carries a risk of intracerebral hemorrhage and requires strict evaluation of contraindications. For acute ischemic stroke patients exhibiting occlusion affecting the large arteries of the brain's anterior circulation, mechanical thrombectomy is recommended within a 24-hour time window from onset (Emberson et al. 2014; Furlan 2015).

There are two major challenges limiting the widespread clinical application of mechanical thrombectomy. First, only roughly 10% of acute ischemic stroke patients eligible for thrombectomy arrive within the 6-hour window suitable for the procedure, while around 9% of patients become eligible for thrombectomy within the 6-24 hour window (Chia et al. 2016). Second, few stroke centers possess the required infrastructure and specialized skills to carry out this procedure, and medical resource constraints hinder its broad clinical application (Sheth et al. 2015).

1.2.1 Pathophysiology of ischemic stroke

With rapid advancements in research on cerebral ischemia pathology and treatment, there is now a clearer understanding of the damage and spontaneous repair mechanisms throughout the progression of ischemic stroke. At the beginning of cerebral ischemic events, the brain is highly sensitive to local ischemia. Interruption of glucose and oxygen

supply leads to neuronal metabolic failure and a cascade of harmful cellular events that ultimately cause rapid neuronal death (Dirnagl, Iadecola, and Moskowitz 1999; Mehta, Manhas, and Raghubir 2007). Preconditioning before ischemia or after ischemia lessens ischemic injury in experiments. However, the clinical translation has been disappointing. The main limitation for these treatments is their very narrow therapeutic window of just minutes to hours around the ischemic event, which makes clinical trials very difficult.

And there is new evidence that shows that the injury of cell in ischemic stroke not only happens at the acute stage but also it will progress to the subacute stage. After ischemia, both apoptosis and neuroinflammatory responses like microglial activation, secreting inflammatory mediators and calling for peripheral immune cells make ischemic harm worse and lead to neuronal loss in the ischemic penumbra. While neuronal loss within the infarct core primarily is a consequence of necrosis, postponed neuronal loss in the ischemic penumbra is largely due to apoptosis (Mattson, Culmsee, and Yu 2000; Mehta, Manhas, and Raghubir 2007). Studies have shown that genes encoding caspases and Bcl family proteins are upregulated in both early and late phases of ischemic stroke. Additionally, inhibiting caspase-3 and caspase-8 or increasing the expression of the anti-apoptotic protein Bcl-2 significantly reduces ischemic injury (Mehta, Manhas, and Raghubir 2007; Zhao et al. 2003).

Neuroinflammation significantly contributes to the development of ischemic stroke, and blocking inflammation effectively reduces ischemic brain damage (Barone and Feuerstein 1999; Dirnagl 2004). Proinflammatory molecules, notably tumor necrosis factor-α (TNF-α), contribute to injury aggravation following ischemia and are released by activated glial cells and neurons (Jin, Yang, and Li 2010). Moreover, peripheral immune cells are key players in the post-ischemic inflammatory response through their secretion of proinflammatory molecules, potentially worsening the condition. Extensive research including animal models of ischemic stroke demonstrated that the inhibition of proinflammation cytokines can lessen the ischemic injury of the brain (Jin, Yang, and Li 2010).

Additionally, ischemic stroke triggers a quick surge in producing chemokines (Basic Kes et al. 2008). Infiltration of peripheral leukocytes, especially neutrophils, and enhancement of BBB permeability and MMPs are mediated by these chemokines, thus worsening injury (Jin et al. 2013; Wang et al. 2012).

Beyond the acute phase, neurons from other parts of the brain adapt to compensate for the lost functions of the ischemic area, a process observable weeks after onset (Wieloch and Nikolich 2006). Also, various post-stroke repair processes such as angiogenesis, neurogenesis, and oligodendrogenesis, have been suggested to be highly complex and dynamic (Cramer 2008; Font, Arboix, and Krupinski 2010; Zhang, Chopp, and Zhang 2013). Pharmacological interventions or rehabilitation therapies can improve outcomes (Koh and Park 2017). Ischemic stroke management is mainly about stopping secondary harm and neuroinflammation, lengthening the time for intervention, and improving recovery by angiogenesis, neurogenesis, oligodendrocytes formation and reestablish neural networks.

1.3. Microglia

Microglia act as the brain's resident phagocytic cells and are essential for initiating innate and adaptive immune responses (Rayasam et al. 2018; Greter, Lelios, and Croxford 2015). According to current research, microglia arise in early macrophage precursors in the yolk-sac of the embryo and live in the brain throughout life; they are involved in the development and maintenance of neurons (Sabogal-Guaqueta et al. 2020).

1.3.1 Microglial morphology

Microglial morphing is very plastic. When there's no inflammation, microglia take on a ramified form, featuring a small cell body and many slender, extensively branched processes that constantly monitor their environment. When pathologically stimulated, microglia take on an amoeboid form characterized by a swollen soma and processes that are shorter and more robust (Tsukahara et al. 2020; Green and Rowe 2024). The changes

at the morphological level seem to give indication of an active state of microglia. It must be pointed out that changes in the morphology of microglia are not always in line with the alterations in function (Green and Rowe 2024).

1.3.2 Microglial polarization

In terms of its function, microglia can take on different functional forms, which can go from being more pro-inflammatory (often referred to as M1) to an anti-inflammatory, tissue-repairing profile (commonly termed M2). Local changes in extracellular and intracellular signaling dictate the phenotypic switch and functionality of microglia (Devanney, Stewart, and Gensel 2020). M1 linked to pro-inflammatory activity has a generation of pro-inflammatory mediators raised. Microglia can be classically activated into this state through lipopolysaccharide (LPS) (Tschoe et al. 2020). As for M1 microglia, its main function is antigen presentation and pathogen removal under homeostatic conditions. But, if activated for a long time or with stimuli, it will cause inflammatory reaction, exacerbate neuroinflammation and lead to neuronal death (Liu et al. 2020). Conversely is M2 microglia which is also called alternatively activated microglia, and it has neuroprotective and anti-inflammatory properties (Walker and Lue 2015).

1.4. Microglia in ischemic stroke

After ischemic stroke, brain suffers from an ischemic cascade and second brain injury. Ischemic neuroinflammatory responses are viewed as a main cause to the second damage (Jurcau and Simion 2021). After cerebral ischemia, the body initiates immune responses to regulate inflammation in the affected brain areas. This response is characterized by the infiltration of various inflammatory cells. The disruption of the blood-brain barrier (BBB) by ischemia allows these immune cells from the bloodstream to enter the ischemic region. Peripheral immune cell infiltration within the CNS creates more neurotoxic mediators and worsens neuroinflammation (Endres et al. 2022). But these immune cells mainly accumulate around blood vessels instead of entering the brain tissue through glial networks. In contrast, microglia quickly get activated and take an important part in

organizing the immune response within the injured brain (Jia et al. 2021). Though there may be similarities in inflammatory responses of infiltrating immune cells and resident microglia, the research indicates that microglia play the larger role following ischemia. (He et al. 2020).

Microglia activation following ischemic stroke plays a paradoxical role, exhibiting either neurotoxic or neuroprotective phenotypes depending on the disease timeline. Current research mainly deals with microglia-induced neuroinflammation, and the damage caused by ischemic stroke. When ischemia occurs, activated microglia would release various inflammatory mediators. This would drive inflammation thereby exacerbating brain injury (Lindhout et al. 2021). And new evidence show that microglia are significant for neuroprotection including immune defense, repair, and regeneration (Wang et al. 2018).

1.4.1 Microglia and neuroinflammation

Accumulating evidence indicates that microglia drive ischemic brain injury by increasing neuroinflammation (Al Mamun et al. 2020). The activation of microglia will occur 1 hour post ischemia and continue for several days. Microglial phenotypic transition of ischemic stroke is also one of the commonly discussed points. Though debated by some neuroscientist, microglia phenotypes are categorized into pro-inflammatory M1 and anti-inflammatory M2 phenotypes. M1 microglia release pro-inflammatory factors which causes neuronal damage (Ye et al. 2019). These factors regulate molecules associated with inflammation and neuronal degenerative. It is through the release of cytokines, chemokines, free radicals, excitotoxic molecules which then indirectly cause neuronal apoptosis while enzymes such as MMPs cause neurons toxicity and cell death (Jurcau and Simion 2021).

1.4.2 Neuroprotective functions of microglia

Following ischemia, microglia rapidly undergo morphological changes to adapt to the altered brain environment. While there was abundant research over the last decades concerning the neurotoxic effect of microglia on ischemic stroke, their neuroprotective

roles remain less understood. Ischemia-induced M2 microglia are regarded as pro-repair due to their involvement in tissue remodeling via debris clearance, inflammation reduction, and production of trophic molecules in large quantities(Berglund et al. 2020; Han et al. 2021; Miron et al. 2013). Also, they respond with the astrocytes to immune responses to limit acute ischemic injury (Kim and Son 2021). In later stages of stroke, active microglia encourage neuronal plasticity and are significant for ischemic restoration (Sandvig et al. 2018).

1.4.3 Targeting microglia in ischemic stroke therapy

Targeting both microglial activity and the associated inflammatory response maybe a promising therapeutic strategy. Although microglia can be a "double-edged sword" in this regard, most clinical study reports mainly focus on microglia inflammation. Recent studies indicate that modulating microglia-mediated neuroinflammation could be a promising strategy (Xue et al. 2021). Microglia are first-line immune defense system and removing them is ineffective for treating ischemic damage. Instead, strategies aimed at lowering M1 microglial activation while encouraging M2 polarization may aid neurological recovery post-stroke. Certain phytochemicals can modulate microglial inflammation by promoting a shift in the M1/M2 polarization balance towards the protective M2 subtype (Subedi and Gaire 2021). Therefore, tightly controlling microglial activation states over time could be a viable therapeutic strategy against ischemic stroke (Jayaraj et al. 2019).

1.5. Chemokine

Chemokines are a kind of small peptide molecules which control the direction of cell migration. It is an arrangement consisting of about 70–100 amino acid sequences: folded structure stabilized by the disulfide bond. There are nearly 50 identified members within the chemokine family, which is a major branch of cytokines. Chemokine receptors act mostly by coordinating intercellular dialogues and immune regulations, which drive chemotaxis and inflammation proliferation (Hughes and Nibbs 2018).

Chemokine receptors belong to the class A GPCR family with a conserved seven-transmembrane domain that facilitates G-protein signaling (Kufareva, Salanga, and Handel 2015). Chemokines elicit reactions on the cell surface by connecting to chemokine receptors. A more detailed view recognizes that chemokine functions are far broader and more powerful than previously thought. They are not simply classic inducers of directional migration with a single pro- or anti-protective effect.

Chemokines are divided into four groups—C, CC, CXC, and CX3C—based on their N-terminal cysteine patterns. The C chemokines contain just one cysteine. The CC chemokines (β-chemokines) feature two adjacent cysteines with no intervening amino acid. The CXC chemokines (α-chemokines) feature two cysteines separated by a single amino acid, whereas the CX3C chemokines have two cysteines with three amino acids in between. In short, these families differ in the number of N-terminal cysteines and the spacing between the first two residues, which underlies their structural and functional diversity (Miller and Mayo 2017; Hughes and Nibbs 2018).

Among these, CC and CXC chemokines are primary chemokines directly linked to stroke pathology. CXC chemokines mostly affects neutrophils, then T cells, while CC chemokines have broader immune cell targets (Hwang et al. 2005).

1.5.1 CCL17

CCL17 binds specifically to CC chemokine receptor 4 (CCR4) and takes an essential part in mediating immune cell migration and inflammatory responses (Hughes and Nibbs 2018). Hippocampal neurons are the principal site for CCL17 expression in the CNS, and CCR4 is broadly expressed on astrocytes and microglia (Fulle et al. 2018; Flynn et al. 2003). CCR4 was first identified in human basophilic cell lines before demonstrating high levels of expression across different types of immune cells, such as Tregs, monocytes, and microglia (Anderson et al. 2020). CCR4-deficient mice exhibit clear behavioral abnormalities, indicating this receptor's role in regulating neuronal and glial functions (Chang et al. 2016; Fulle et al. 2018). Although the CCL17/CCR4 axis has been

extensively studied in immune and inflammatory responses, its exact function in ischemic stroke is still unknown. But recently Yvonne et al. found that CCL17 promotes atherosclerosis by signaling through CCR8, rather than CCR4, to induce CCL3 expression and suppress Treg function, revealing a non-canonical chemokine pathway that impairs atheroprotection (Yvonne et al. 2024).

1.6. Diverse cell death in the ischemic penumbra

In the ischemic penumbra, neurons experience multiple types of cell death (Fricker et al. 2018). Among them, necroptosis is a controlled form of necrotic cell death that combines features of apoptosis and necrosis and is particularly implicated in ischemic stroke (Hribljan et al. 2019; Liu et al. 2018). Nevertheless, apoptosis remains predominant in the ischemic penumbra (Broughton, Reutens, and Sobey 2009; Hankey 2017; Iadecola and Anrather 2011; Mehta, Manhas, and Raghubir 2007; Onteniente et al. 2003; Puyal, Ginet, and Clarke 2013; Yao et al. 2001).

The ischemic penumbra exhibits spatial heterogeneity**.** Electron microscopy of the cortical penumbra in rats reveals a graded pathological pattern: tissue degeneration is most severe near the infarct core and diminishes towards the periphery (Uzdensky 2018). Directly surrounding the necrotic core lies a narrow transitional zone with critically low ATP levels, which exhibits features of both necrosis and apoptosis (Mehta, Manhas, and Raghubir 2007). In the larger surrounding penumbral area where ATP levels are moderately higher, apoptotic cell death becomes the dominant mechanism. Temporally, necrosis develops within minutes of stroke onset, while apoptosis evolves over subsequent hours to days.

In contrast to the inevitable and unregulated nature of necrotic cell death, apoptosis is a controlled process amenable to pharmacological intervention. This functional dichotomy establishes the ischemic penumbra—where apoptosis prevails—as a prime target for neuroprotection, making its inhibition a compelling therapeutic strategy for stroke

(Broughton, Reutens, and Sobey 2009; Ferrer 2006; Fricker et al. 2018; Nakka et al. 2008; Radak et al. 2017).

There is no clear anatomical boundary between the necrotic infarct core and the ischemic penumbra, where cell death is ongoing. Ultrastructural and biochemical analyses occasionally reveal apoptotic features within the infarct core, a region conventionally regarded as necrotic (Onteniente et al. 2003). Conversely, within the ischemic penumbra, multiple types of cell death occur in the ischemic region. Some cells exhibit morphological and biochemical features indicative of both apoptotic and necrotic processes**,** such as caspase-3 activation (Ferrer et al. 2003; Onteniente et al. 2003; Yao et al. 2001). Furthermore, cells undergoing necroptosis have also been identified in the ischemic penumbra (Fricker et al. 2018).

1.7. Apoptosis

Across diverse animal species, apoptosis functions as a conserved and strictly regulated pathway of programmed cell death and has been a focal point of decades of systematic research, particularly in the last thirty years. For much of this period, apoptosis was thought the only mechanism of regulated cell death. A key feature of apoptosis is the mitochondrial release of cytochrome c as well as the activation of initiator caspases (caspase-8, -9, and -10) and effector caspases (caspase-3, -6, and -7). The execution of apoptosis culminates in nuclear envelope disintegration mediated by caspase-6, proteolytic cleavage of key intracellular substrates such as poly (ADP-ribose) polymerase (PARP) and lamin, plasma membrane blebbing, and fragmentation of genomic DNA into nucleosomal units (Fraser and Evan 1996; Nicholson and Thornberry 1997). These molecular and morphological features serve as canonical indicators of apoptosis and are commonly employed to delineate the specific cell death pathways involved, including DNA fragmentation and the activation of executioner caspase-3 together with PARP cleavage.

1.7.1 Intrinsic apoptosis

Apoptosis can proceed through two distinct, non-exclusive pathways: the intrinsic and extrinsic pathways(Vogler et al. 2025). The regulation and coordination of both processes rely on a specific group of proteases known as caspases. Caspases do not, however, appear to function as death factors per se; rather, they seem to intensify and accelerate the apoptotic signal, primarily to curtail its immunogenic potential (Riedl and Shi 2004). MOMP, mitochondrial outer membrane permeabilization, is an essential part of the intrinsic pathway and is regulated by BCL-2 family proteins (Newton et al. 2024). Pro-apoptotic proteins accumulate on the outside of the mitochondrial membrane to form pores from which the pro-apoptosis elements, such as second mitochondria-derived activator of caspases (SMAC) and cytochrome c, exit and enter the cell. On the other hand, anti-apoptotic BCL-2 proteins prevent the pro-apoptotic process (Kalkavan and Green 2018). Susceptibility of cells to apoptosis is regulated by the dynamic balance between these two opposing forces. BCL-2 inhibitors, such as gossypol and ABT-199, promote apoptosis in cancer cells by disrupting the protective effects of anti-apoptotic factors, thereby tipping the balance toward cell death (Tait et al. 2010). Once MOMP occurs, cells generally pass a point of no return, although some exceptions have been reported (Gong et al. 2019). Although intrinsic apoptosis requires MOMP, it does not totally depend on caspase activity, because the cell dies after MOMP whether caspases are on or off. Caspase activation upon MOMP just accelerates the process (Kalkavan and Green 2018), thereby enabling the host to efficiently clear apoptotic bodies and prevent immune response (Arandjelovic and Ravichandran 2015). Yet cells still dye after MOMP, even when caspase activity is blocked. Under these circumstances, a dying cell release signals and tells its host to respond.

1.7.2 Extrinsic apoptosis

Extrinsic apoptotic pathway is activated when pro-apoptotic receptors on cells become active after they bond pro-apoptotic molecules and ligands. The death receptors (DRs) belong to the tumor necrosis factor (TNF) receptor family, and include the most studied

members such as the Fas receptor and TNFR1 (Ghobrial, Witzig, and Adjei 2005). The Fas receptor is expressed on various cell types, including activated B cells and T cells (Wajant 2003). Ligands that activate these pro-apoptotic receptors include Fas ligand (FasL) and TNF-α (Golks et al. 2006; Gomez-Angelats and Cidlowski 2001; Imtiyaz, Zhang, and Zhang 2005; Lavrik, Golks, and Krammer 2005a; Sandu et al. 2005; Wajant 2003). FasL is produced predominantly by activated T cells and natural killer cells (Green and Ferguson 2001). In contrast, TNF-α secretion is largely attributed to activated monocytes/macrophages (Riches, Chan, and Winston 1996).

Death receptors contain a conserved cytoplasmic death domain (DD). When the ligand binds to its receptor and the receptors cluster, these DDs come into proximity, building a platform for adaptor to join in. Each receptor selects its own adaptor—Fas-associated DD (FADD) for Fas and TNF receptor-associated DD (TRADD) for TNFR1. The death-inducing signaling complex (DISC), consisting of the ligand, receptor, and adapter proteins, is a scaffold for the recruitment and assembly of caspase-8 and -10 (Scott et al. 2009). Via autocatalytic cleavage, recruited initiator caspases release their active subunits into the cytoplasm. These active subunits then activate downstream effector caspases 3, 6, and 7 (Ashkenazi 2002; Ghobrial, Witzig, and Adjei 2005; Lavrik, Golks, and Krammer 2005b).

However, in hepatocytes, stimulating the extrinsic pathway by itself will not trigger apoptosis; amplification loop by the intrinsic pathway is required (Kalkavan and Green 2018). Caspase-8 converts BID into tBID in these cells, which in turn activates BAK/BAX-driven MOMP. The bridge between the cell-surface death signal pathway and the mitochondrial pathway ensures that apoptosis can proceed efficiently even when external death signals fail to cause cell death (Haudek et al. 2007; Jost et al. 2009).

1.8. The aim of the study

Ischemic stroke induces neuronal loss and neuroinflammation which involve microglial polarization. M1 microglia exert pro-inflammatory effects, whereas M2 microglia

promote reparative and neuroprotective functions. CCL17 is a kind of chemokine previously recognized for its role involved in regulation of immune systems and recruiting Treg cells, but recent research points out its ability to change neuroimmune reaction. However, its role in ischemic stroke, especially in microglia polarization and neuron survival is still poorly understood. This study investigates whether recombinant CCL17 (rCCL17) can modulate microglial phenotype under ischemic and inflammatory conditions. It also explores the direct protective effects of rCCL17 on primary neurons exposed to hypoxic stress, and whether rCCL17-pretreated microglia enhance neuronal viability, possibly by reducing neuronal apoptosis.

2. Materials and methods

2.1. Materials

Table 1: Equipment

Instrument	Manufacture
Biological cabinet	NuAire, USA
Thermocycler	Analytik Jena GmbH, Germany
ChemoCam Imager	INTAS, Germany
Power supply	Avantor, USA
pH meter	Hanna Instruments, USA
Refrigerated Centrifuge	Hettich GmbH, Germany
Inverted microscope for cell culture plates	A. KRÜSS Optronic GmbH, Germany
Mikro 120 Tabletop centrifuge	Andreas Hettich GmbH, Germany
Microplate photometer	Thermo Fisher, USA
Thermal Cycler System	Bio-Rad, USA
NanoPhotometer P330	Implen GmbH, Germany
Counting chamber	Glaswarenfabrik Karl Hecht, Germany
Peristaltic pump	Carl Roth, Germany
Pipettes	Various companies
QuantStudio3 PCR System	Thermo Fisher, USA
Refrigerators and freezers	Various companies
Roller RM5 Assistent 348	Glaswarenfabrik Karl Hecht, Germany
Vortex-Genie 2	Thermo Fisher, USA
Semi-dry transblotting cell	Bio-Rad, USA
Water bath	Memmert, Germany
Weighing balances	Sartorius Stedim Biotech, Germany

Table 2: Lab consumables

Item	Manufacture
Cell scraper	Greiner, Germany

60 mm dish	Greiner, Germany
6 well plate 24 well plate Flat bottom lid TC-Plate 96 well sterile	Greiner, Germany
Cell culture flask 25 cm^2 Cell culture flask 75 cm^2	Greiner, Germany
70 µm Cell Strainer	Corning, USA
6 well transparent PET Membrane	Greiner, Germany
Glass Pasteur pipettes 150 mm	BRAND, Germany
Microscope cover slips	Glaswarenfabrik Karl Hecht, Germany
Filters (0.2 µm)	Sartorius AG, Germany
Mr. Frosty™ freezing container	Thermo Fisher, USA
PVDF membrane 0.45 µm	Thermo Fisher, USA
PVDF membrane 0.2 µm	Carl Roth, Germany
Parafilm	Merck KGaA, Germany
Pipette tips (pyrogen and DNase free) 10 µl; 20 µl; 100µl; 200 µl; 1000 µl	nerbe plus GmbH & Co. KG, Germany
Pipette tips standard 10 µl; 20 µl; 100µl; 200µl; 1000 µl	Sarstedt AG & Co. KG, Germany
Plastic pipettes: 5 ml; 10 ml; 25 ml	Greiner Bio-One, Germany

Table 3: Chemical

Compound name	**Manufacture**
Ammonium persulfate (APS)	Carl Roth, Germany
B-27™ Supplement	Thermo Fisher Scientific, USA
Bovine Serum Albumin (BSA)	Capricorn Scientific GmbH, Germany

Compound name	**Manufacture**
Calcium Chloride ($CaCl_2$)	Carl Roth, Germany
3-(4,5-Dimethyl-2-thiazolyl)-2,5-diphenyl-2H-tetrazolium Bromide (MTT)	Merck KGaA, Germany
4',6-Diamidino-2-phenylindol dihydrochloride (DAPI)	Thermo Fisher, USA
DMEM/Ham'sF-12 (DMEM/F-12)	Capricorn Scientific GmbH, Germany
Dipotassium phosphate (K_2HPO_4)	Carl Roth, Germany
Disodium phosphate (Na_2HPO_4)	Carl Roth, Germany
Dulbecco's Modified Eagle Medium (DMEM)/F-12	Thermo Fisher, USA
Dimethyl sulfoxide (DMSO)	Carl Roth, Germany
Dulbecco's phosphate buffered saline (DPBS) 10X	Carl Roth, Germany
Ethanol 100%	Merck KGaA, Germany
Fetal bovine serum (FBS)	Thermo Fisher, USA
Recombinant Mouse CCL17/TARC Protein	R&D Systems, USA
Lipopolysaccharides (LPS)	Sigma Aldrich, USA
Glucose	Carl Roth, Germany
Glycine	Merck KGaA, Germany
GlutaMAX Supplement	Thermo Fisher, USA
Hanks' Balanced Sait Solution (HBSS) (10X)	Thermo Fisher, USA
HEPES Buffer Solution(1M)	Thermo Fisher, USA
HEPES powder	Merck KGaA, Germany
Hydrochloric acid 37%	Merck KGaA, Germany
Isoflurane 100%	Ecuphar, Germany
ITS supplement(100X)	Carl Roth, Germany
Magnesium sulfate ($MgSO_4$)	Carl Roth, Germany
Methanol	Merck KGaA, Germany
3-Methyladenine(3-MA)	Merck KGaA, Germany

Compound name	**Manufacture**
Neurobasal Medium	Thermo Fisher, USA
Neuron Isolation Enzyme (with papain)	Thermo Fisher, USA
Protein Ladder	Thermo Fisher, USA
Penicillin/Streptomycin (P/S)	Thermo Fisher, USA
PBS-Puffer (10X Dulbecco)	Altmann Analytik, Germany
Paraformaldehyde (PFA)	Merck KGaA, Germany
Phosphatase inhibitor cocktail 2	Merck KGaA, Germany
Poly-D-lysine (PDL) Gibco™	Thermo Fisher, USA
Potassium chloride (KCl)	Carl Roth, Germany
ProLong Glass Eindeckmittel	Thermo Fisher, USA
Protease inhibitor cocktail	Roche, Germany
RIPA Lysis and Extraction Buffer	Thermo Fisher, USA
ROTI Load1	Carl Roth, Germany
Gel 30% acrylamide mix	Carl Roth, Germany
Sodium dodecyl sulfate (SDS)-polyacrylamide gel electrophoresis PAGE 10X	Carl Roth, Germany
Sodium dodecyl sulfate (SDS)	Carl Roth, Germany
Sodium Bicarbonate ($NaHCO_3$)	Merck KGaA, Germany
Sodium carboxymethyl cellulose	Merck KGaA, Germany
Sodium chloride (NaCl)	Carl Roth, Germany
Sodium hydroxide (NaOH)	Merck KGaA, Germany
Tetramethyl ethylenediamine (TEMED)	Carl Roth, Germany
Trishydroxymethyl aminomethan (Tris)	Carl Roth, Germany
Tris-HCl	Carl Roth, Germany
Triton X-100 (10%)	Merck KGaA, Germany
Trypan blue	Carl Roth, Germany
Trypsin (2.5 g/l)	Thermo Fisher, USA
Tween 20	Merck KGaA, Germany

Table 4: Kits

Kits	Manufacturer	Cat. No	Method
DC Protein Assay Kit	Bio-Rad, USA	5000113	Protein quantification
ECL substrate	Thermo Fisher, USA	34580	Western Blot
First Strand cDNA-Synthese-Kit	Thermo Fisher, USA	K1652	Reverse Transcription
SYBR Green Master Mix	Applied-Bio, USA	A25776	Polymerase Chain Reaction (PCR)

Table 5: Buffers

Buffer Name	Ingredients	Amount
APS	H_2O APS	10 ml 1 g
Blocking buffer	TBST BSA	100 ml 5 g
Running Buffer	H_2O SDS-PAGE 10X	1800 ml 200 ml
SDS solution	H_2O SDS	10 ml 1 g
TBS 20X	H_2O NaCl Tris	1000 ml 175.4 g 48.2 g
TBST 1X	TBS 20X Tween H_2O	50 ml 1 ml 950 ml
Transfer Buffer	H_2O Methanol SDS-PAGE 10X	1400 ml 400 ml 200 ml

Buffer Name	Ingredients	Amount
BSS0 10x stock solution	ddH_2O	800 ml
	NaCl	68 g
	KCl	4 ml
	$MgSO_4$	2 g
	$NaH_2PO_4•H_2O$	1.4 g
BSS0 1x solution	ddH_2O	43 ml
	10x BSS0	50 ml
	1 M $NaHCO_3$	13.1 ml
	1 M HEPES	5 ml
	30 mM Glycine	166 µl
	1 M $CaCl_2$	900 µl
DPBS	ddH_2O	100 ml
	DPBS	900 ml
Poly-D-lysine (PDL)	DPBS	100 ml
	Poly-D-lysine	100 ml
Neurobasal medium	Neurobasal medium (1X)	500 ml
	B27 Supplement (2%)	10 ml
	Transferrin (5 µg/ml)	500 µl
	L-glutamine (0.5 mM)	250 µl
	1xPen-Strep (1%)	5 ml

Table 6: Primary Antibodies

Name	Host	Dilution	Method	Art.No	Manufacture
IBA-1	Rabbit	1:500	IF	ab178846	Abcam
CD206	Mouse	1:500	IF	MA5-16871	Thermo Fisher
β-actin	Rabbit	1:1000	WB	ab8227	Abcam
Caspase 3	Rabbit	1:1000	WB	4108	Cell Signaling

Table 7: Secondary Antibodies

Antibody	Host	Dilution	Art. No	Manufacturer
Goat Anti-Rabbit IgG H&L (HRP)	Goat	1:10000	ab6721	Abcam
Goat anti-Rabbit IgG Secondary Antibody, Alexa Fluor™ 488	Goat	1:500	A11008	Cell Signaling Technology
Goat anti-Mouse IgG Secondary Antibody, Alexa Fluor™ 555	Goat	1:500	A21422	Thermo Fisher

2.2. Methods

2.2.1 Isolation of primary microglia

In brief, this workflow consists of two main parts: isolation of the mouse cortex and processing the cortex into a single-cell suspension. Prepare chilled HBSS and ice packs before the operation. Pay attention to the temperature during the operation and replace the HBSS frequently. First, remove the head of the P1-P3 C57BL/6J pups, and then use scissors to cut the scalp and soft skull along the sagittal suture. Take out the entire brain tissue and quickly place it in a 60 mm dish. Then pour in HBSS to slightly immerse the tissue and make it easy to flip with tweezers under a surgical microscope. The cerebellum and olfactory bulbs were excised with a sterile blade, and the meninges were removed under microscope. Cortices were then separated using forceps and transferred into a 15 ml tube containing 300 µl of Neuron Isolation Enzyme with papain for digestion at 37 °C for 30 minutes. Subsequently, the suspension was spun down (1400 Revolutions Per Minute (RPM), 5 minutes, room temperature (RT)). Cells were plated in PDL-coated T75 flasks and maintained at 37 °C with 5% CO2. Debris was removed by replacing the culture medium on the following day, with subsequent medium changes performed every five days. By 5–7 days in vitro, astrocytes had developed into a confluent adherent layer, supporting the growth of microglia above them. To isolate microglia, the culture flasks

were tapped to dislodge the loosely attached cells, and the resulting suspension was harvested as an enriched microglial fraction.

2.2.2 Isolation of primary neurons

Culture plates were coated with PDL (0.1 mg/ml; 2 ml per well for six-well plates, 0.5 ml per well for 24-well plates) and incubated at RT for at least 1 hour. After rinsing three times with sterile ddH_2O, the plates were air-dried and stored until further use.

On embryonic day 16.5, dams were humanely euthanized with isoflurane. Embryonic brains were isolated under sterile conditions, and the meninges were carefully removed. Cortices and hippocampi were collected and placed in 15 ml tubes containing ice-cold HBSS. After removal of HBSS, the tissue was digested with Neuron Isolation Enzyme at 37°C for 30 minutes, with gentle shaking every 10 minutes. Digestion was terminated by adding 2 ml of Neurobasal medium (components are shown in **Table 5**). The tissue was homogenized by pipetting 5-10 times. Wait 1 minute to allow the tissue fragments to settle and transfer the supernatant containing the single-cell suspension to a 15 ml centrifuge tube. To further enhance cell yield, the remaining fragments were homogenized again in 2 mL of Neurobasal medium. Following centrifugation (600 rpm, 5 minutes), the supernatant was removed, and the resulting cell pellet was mixed in Neurobasal medium for subsequent cell quantification. Cells were seeded at densities of one million cells/well for 6-well plates and 200,000 cells/well for 24-well plates. The cultures were maintained under standard conditions (5% CO_2, 37°C). After 4 h, the medium was replaced to remove debris. The primary neurons were then cultured for an additional 5-7 days ahead of further experimental procedures.

2.2.3 Oxygen-glucose deprivation (OGD) model

Prior to OGD treatment, primary neurons were cultured for 5–7 days until reaching 80–90% confluency, whereas primary microglia were subjected to hypoxic treatment 1–2 days after seeding. After two DPBS washes, cells were incubated in BSS0. Cells were transferred to a hypoxia chamber and incubated under hypoxic conditions (1.5% O_2, 5% CO_2, 45% humidity, 37°C) for a predetermined duration. After OGD, cells were rinsed

with DPBS and returned to their respective culture media. Reoxygenation (R) was performed under normoxic conditions (5% CO_2, 37°C) for 24 h. Subsequent analyses were conducted as required, depending on the experimental design.

2.2.4 Drug treatment

Primary microglia were serum-starved in DMEM containing 1% P/S for 2 h prior to treatment. For experiments under hypoxic conditions, Cells were treated with increasing amounts of CCL17 (50, 100, and 150 ng/ml) as indicated and incubated overnight prior to OGD/R induction the following day. For experiments involving LPS stimulation, microglia were incubated with 150 ng/ml CCL17 and 1 μg/ml LPS.

For primary neurons, CCL17 was applied at the specified concentrations (50, 100, or 150 ng/mL) during the reoxygenation period.

2.2.5 Co-culture system of primary neurons and microglia

Microglia were seeded into 0.4 μm transwell inserts, while neurons were maintained in the lower wells. Both cell types underwent OGD/R modeling following the same protocol as described in the drug treatment section. The timing was coordinated such that microglia completed reoxygenation just as neurons began reoxygenation. At this point, transwell inserts containing microglia were transferred to the neuronal wells for co-culture, which was maintained for 24 h. Subsequent analyses included western blotting or MTT assay as required.

2.2.6 Cell survival assay

We used the MTT assay to evaluate cell viability. Active cells reduce tetrazolium salts to purple formazan crystals, forming the basis of this assay. We examined the effects of varying hypoxia lengths (2–8 h) on cell survival and the influence of CCL17 at 50–150 ng/ml on neuronal survival following a set hypoxia duration.

Following OGD/R, cells were incubated with 100 μl of MTT solution (5 mg/ml in PBS) at 37 °C for 4 h. The medium was subsequently discarded, and 1 ml of DMSO was applied

to dissolve the resulting formazan crystals with gentle agitation for 5 minutes. Subsequently, 200 µL of the dissolved solution from each well was transferred to a 96-well microplate for spectrophotometric measurement of absorbance at 570 nm.

2.2.7 Immunofluorescence

We fixed the primary microglia (cultured on coverslips in 24-well plates) with 4% PFA for 10 minutes, permeabilized them with 0.25% Triton X-100 for 5 minutes, and blocked them with 5% BSA at room temperature for 30 min. Cells were then incubated overnight at 4 °C with primary antibodies (**Table 6**), followed by 1 h incubation with fluorophore-conjugated secondary antibodies (**Table 7**) at RT. After counterstaining with DAPI, coverslips were mounted using anti-fade medium and stored at 4 °C until imaging.

2.2.8 RNA isolation and qRT-PCR analysis of primary microglia

2.2.8.1 Total RNA extraction

We extracted RNA from primary microglia following the kit protocol. Briefly, cells were lysed and homogenized in RLT buffer supplemented with 1% β-mercaptoethanol, then combined with an equal volume of 70% ethanol for subsequent isolation. The lysate-ethanol mixture was applied to a RNeasy Mini spin column and centrifuged to bind RNA to the membrane. After the initial flow-through was discarded, columns were rinsed with RW1 buffer and centrifuged again. Two washes with 500 µL of RPE buffer followed, with the final wash centrifuged for 2 minutes to ensure complete drying of the membrane. To elute the RNA, 30 µL of RNase-free water was added directly onto the membrane. The sample was then centrifuged at 8,000 × g for 1 minute. RNA concentration and purity were assessed via a NanoPhotometer P330.

2.2.8.2 Reverse transcription

Total RNA was reverse transcribed into cDNA using the First Strand cDNA-Synthese-Kit (Thermo Fisher, USA, **Table 4**) following the guideline. Briefly, 1000 ng of total RNA was used in a 15 µl reaction mixture (**Table 8**). The components were assembled in

sterile, nuclease-free tubes, briefly spun down, and subjected to incubation at 65 °C for 5 minutes. The tube was then immediately placed on ice and spun again. The next step was adding the components listed in **Table 9** and an incubation at 25 °C for 10 minutes and 50 °C for 15 minutes. The reaction was stopped by heating the mixture at 85 °C for 5 minutes.

Table 8: First-Strand cDNA synthesis

Component	**Volume**
Template	1000 ng
Oligo (dT) 18 primer	0.25 µl
Random hexamer primer	0.25 µl
Water, nuclease-free	Add to 15 µl

Table 9: First-Strand cDNA synthesis

Component	**Volume**
5X RT Buffer	4 µl
Maxima H Minus Enzyme Mix	1 µl
Total volume	To 20 µl

2.2.8.3 Quantitative real-time PCR

Quantitative real-time PCR (qRT-PCR) was carried out with the SYBR Green Master Mix, following the manufacturer's protocol. Each 20 µl of the reaction mixture contained the miRNA-specific forward primer and a universal reverse primer, as detailed in **Table 10**. PCR cycling conditions were carried out according to the standard protocol (**Table 11**), and Table 12 summarizes the primer sequences employed. Gene expression was normalized and analyzed with the comparative ΔΔCT calculation, where ΔCT represents the difference between the target gene and the housekeeping gene, and transcript levels were normalized against β-actin and expressed as 2^−ΔCT values.

Table 10: qRT-PCR reaction setup

Component	**Volume (20µl/well)**
SYBR Green Master Mix	10 µl
Forward and reverse primer (500nM)	2 µl
cDNA template	2 µl
Nuclease-free water	6 µl

Table 11: Standard protocol for qRT-PCR reaction

Step	**Temperature**	**Time**	**Cycles**
Initial Denaturation	95°C	2 minutes	1
Amplification Cycles			
Denaturation	95°C	15 seconds	40
Anneal/extend	60°C	1 minute	
Melt Curve Analysis			
Denaturation	95°C	15 seconds	1
Anneal/extend	60°C	1 minute	
Dissociation	60°C-95°C	0.1 °C/sec	

Table 12: Primers for RT-qPCR analysis

Gene	Primers
CD16	Forward: TTTGGACACCCAGATGTTTCAG Reverse: GTCTTCCTTGAGCACCTGGATC
CD32	Forward: AATCCTGCCGTTCCTACTGATC Reverse: GTGTCACCGTGTCTTCCTTGAG
iNOS	Forward: CAAGCACCTTGGAAGAGGAG Reverse: AAGGCCAAACACAGCATACC
CD206	Forward: CAAGGAAGGTTGGCATTTGT Reverse: CCTTTCAGTCCTTTGCAAGC

Arg-1	Forward: TCACCTGAGCTTTGATGTCG Reverse: CTGAAAGGAGCCCTGTCTTG
IL-10	Forward: CCAAGCCTTATCGGAAATGA Reverse: TTTTCACAGGGGAGAAATCG
β-actin	Forward: GGCTGTATTCCCCTCCATCG Reverse: CCAGTTGGTAACAATGCCATGT

2.2.9 Western blot

2.2.9.2 Protein extraction and quantification

After completing the above treatments, two washes with ice-cold PBS were performed to remove residual medium. The adherent cultures were scraped on ice with a sterile plastic scraper and transferred into precooled 1.5 ml tubes. Cell suspensions were spun down at 2800 RPM for 6 minutes at 4 °C, and pellets were lysed in RIPA buffer containing 1% protease inhibitor cocktail. Cell lysates were kept on ice for 30 minutes with intermittent vortexing to ensure complete lysis. Lysates were centrifuged at 12,000 × g for 20 minutes at 4 °C, and the supernatants containing total soluble proteins were carefully collected and stored at −80 °C for further analysis.

We used DC Protein Assay Kit (Bio-Rad, USA) to determine protein concentrations. Briefly, BSA standards from 0 to 1.4 μg/μL were used to create a standard curve. Each well of a 96-well plate received 5 μL of sample or BSA standard mixed with 25 μL of Reagent A/S, after which 200 μL of Reagent B was added. After incubating for 10 minutes, absorbance was read at 750 nm. Protein concentrations were quantified using the standard curve and all lysates were normalized to the same concentration using RIPA buffer. After mixing with reducing SDS loading buffer, heating at 95 °C for 6 minutes was performed to denature the samples.

2.2.9.3 Western blotting

A 15% SDS-polyacrylamide gel was used to separate equal protein samples (30 µg per lane), appropriate for the target protein's molecular weight. Electrophoresis was performed at 80V for 30 minutes, and then at 120V until the dry front reached the bottom of the gel. Before transfer, PVDF membrane was activated by immersing it in methanol for 3 seconds. A transfer sandwich was prepared by layering filter paper, the gel, the PVDF membrane, and an additional sheet of filter paper, with care taken to remove any air bubbles. Protein transfer was performed by semi-dry blotting at 1.0 A for 15 min. Samples were blocked in TBST with 5% BSA for 30 minutes at RT, then incubated with the primary antibody overnight at 4 °C (**Table 6**). After three washes in TBST next day, the membranes were incubated with a 1:10,000 dilution of secondary antibody for 1 hour at RT. After another three washes with TBST, signal detection was performed by incubating the membrane with ECL substrate, followed by imaging using the INTAS ECL ChemoStar system. Band intensities were quantified using ImageJ software.

2.2.10 Statistical analysis

Data are expressed as mean ± standard deviation (SD). Comparisons among three or more groups were performed using one-way ANOVA followed by Tukey's post hoc test. Statistical analyses and graph preparation were conducted with GraphPad Prism 10 (GraphPad Software, CA, USA), and data handling was carried out in Excel. A p value < 0.05 was considered statistically significant.

3. RESULTS

3.1. Characterization of primary microglia

To verify the successful isolation of primary microglia, cells were carefully analyzed via bright-field imaging. As presented in Figure 1, primary microglial cells exhibit two distinct morphologies: tennis racket-like cells with a round cell body and a single elongated process (green arrow), and rod-shaped cells with an elongated body and processes at both ends (white arrow).

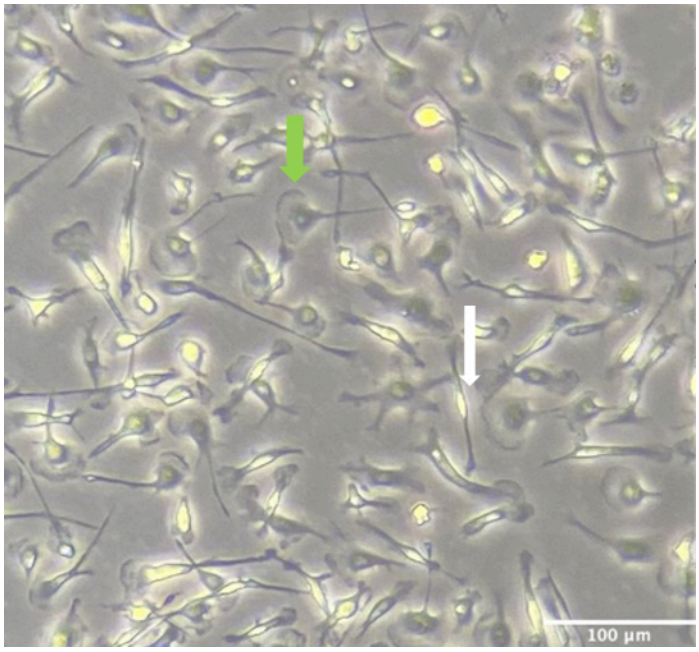

Figure 1. Microglial morphology. Primary microglial cultures were established from P1–P3 C57BL/6J mice. Green arrows indicate tennis racket-shaped microglia, and white arrows indicate rod-shaped microglia.

For purity analysis, immunofluorescence techniques were used, and the microglia cells were stained with two markers, IBA-1 and CD206.

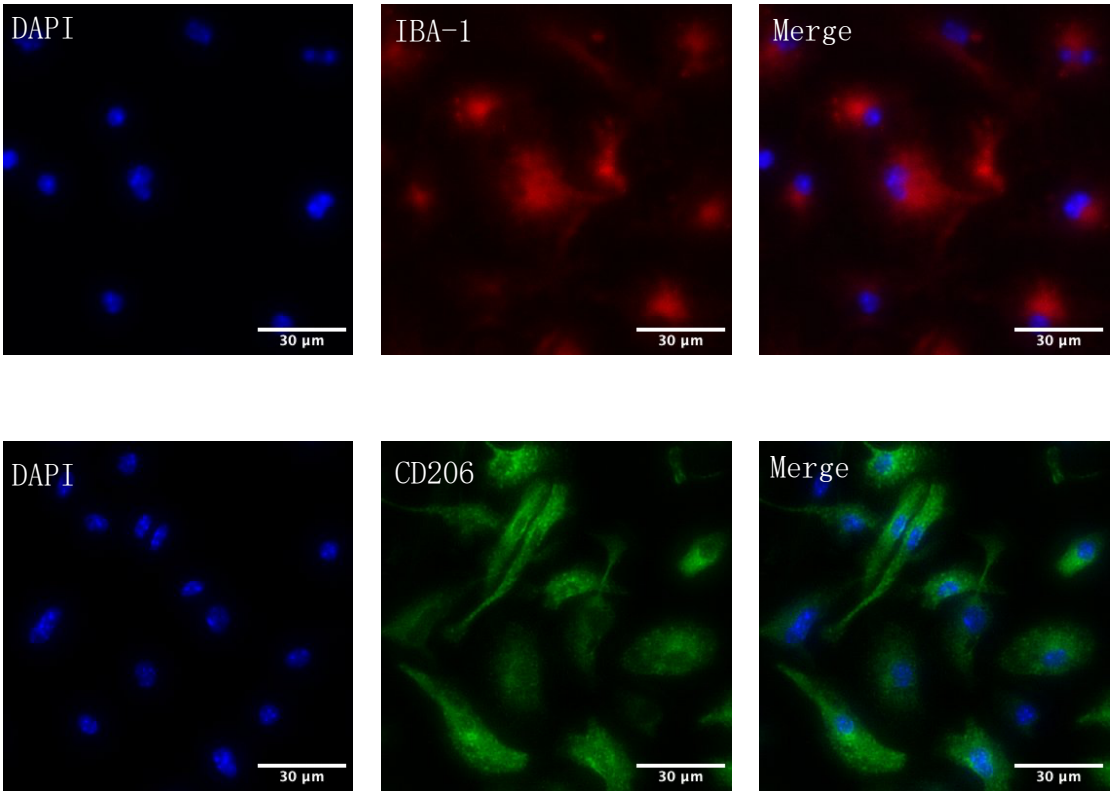

Figure 2. Immunofluorescence characterization of primary microglia. Immunofluorescence characterization of primary microglia under normoxic conditions, stained with the specific microglial markers IBA-1 and CD206. Nuclear counterstaining is shown in blue (DAPI).

To determine cell viability after different hypoxia durations and 24 h reoxygenation, MTT absorbance was quantified in primary microglial cultures. Cells maintained under normoxic conditions served as the control for the viability assay. Figure 3 demonstrates a significant impact of OGD treatment on primary microglial viability. This result showed that after 2 h of OGD the cell viability was already significantly decreased and gradually decreased to around 50% after 4 or 6 h of OGD. A reduction in cell viability of approximately 50 % was considered ideal for further experiments. Based on this, a standard in vitro paradigm of 4 h OGD prior to a 24 h reoxygenation period was established.

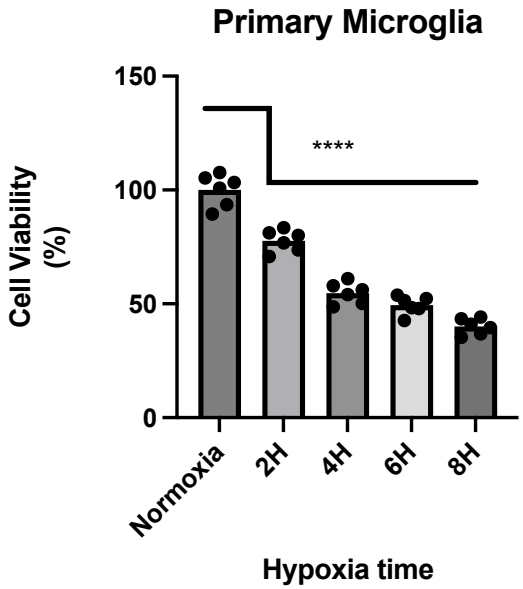

Figure 3. MTT assay for the viability of primary microglia under different durations of hypoxia. Each group included six technical replicates. ****p < 0.0001, ANOVA.

3.2. rCCL17 suppresses M1 microglia polarization and promotes microglia polarization to the M2 phenotype under OGD/R conditions and LPS stimulation

Microglia can shift toward a pro-inflammatory M1 or an anti-inflammatory M2 state. To assess how OGD/R affects this polarization, we quantified canonical M1 markers (CD16, CD32, and iNOS) and M2 markers (CD206, Arg-1, and IL-10) using RT-qPCR. Primary microglial cultures were subjected to various concentrations of rCCL17 (0, 100, and 150 ng/mL) under either normoxic or OGD/R conditions. Analysis of the OGD/R effect alone revealed a substantial upregulation in the transcription of M1 markers (CD16, CD32, iNOS; Figures 4A-C). Conversely, the expression levels of M2 markers (CD206, Arg-1, IL-10; Figures 4D-F) exhibited only a modest, non-significant increase. rCCL17 treatment did not alter the polarization state of microglia under normoxic conditions. However, in the OGD/R context, administration of 150 ng/mL rCCL17 effectively suppressed the OGD/R-triggered M1 polarization (Figures 4A-C) and concurrently enhanced the expression of M2 phenotypic markers (Figures 4D-F). Of note, a significant decrease in CD16 expression was already evident at the 100 ng/mL dose (Figure 4A),

implying that the immunomodulatory actions of rCCL17 may follow a dose-dependent pattern.

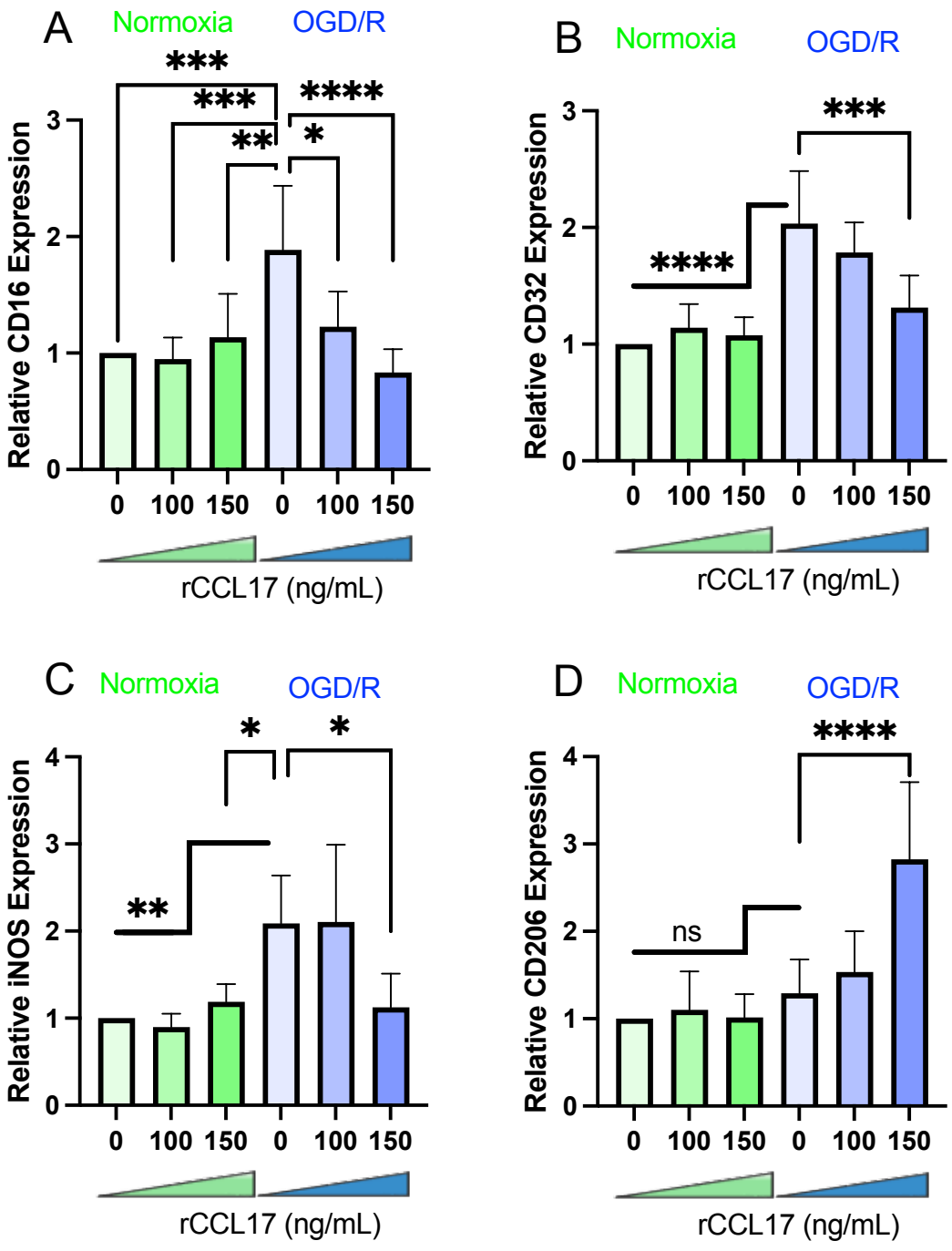

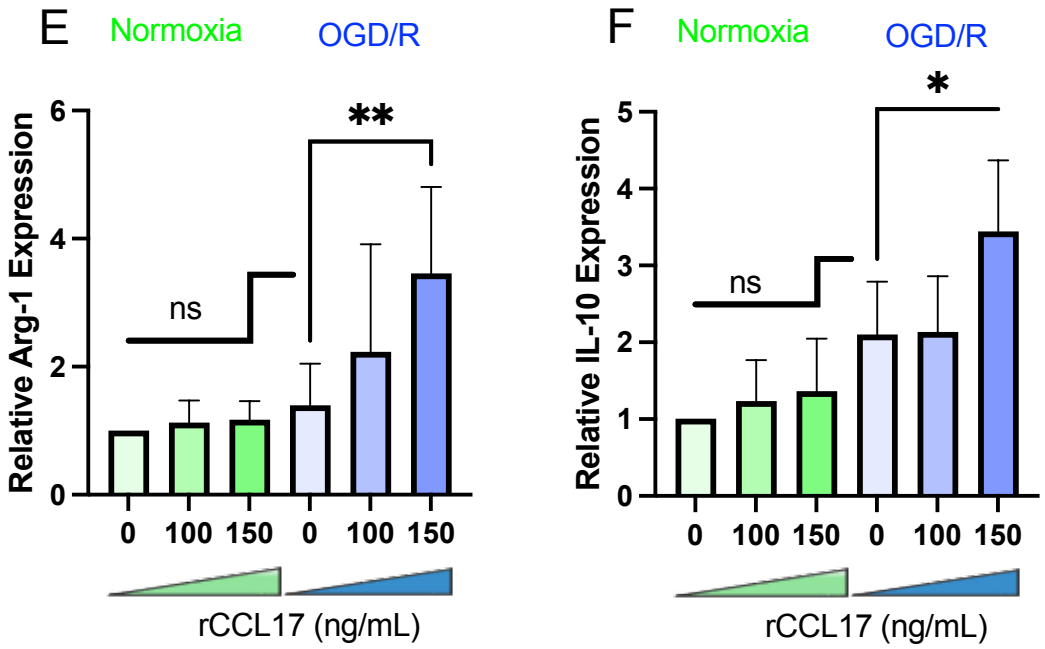

Figure 4. Effect of OGD/R and rCCL17 on microglial polarization. The graph shows RT-qPCR analysis of (A-C) M1 and (D-F) M2 marker gene expression in primary microglia (n=6). ns, not significant; *p < 0.05, **p < 0.01, ***p < 0.001, ****p < 0.0001, ANOVA.

To further explore the anti-inflammatory role of rCCL17, we assessed its effect on LPS-induced microglial polarization. The mRNA expression of M1 (CD16, CD32, iNOS; Figure 5A-C) and M2 (CD206, Arg-1, IL-10; Figure 5D-F) signature genes was compared across control, LPS, and LPS + rCCL17 (150 ng/mL) groups.

As expected, LPS stimulation notably spurred on the M1 phenotype as shown by notable increases in CD16, CD32 and iNOS, but also suppressed the M2 phenotype with reductions in CD206, Arg-1 and IL-10. Treatment with rCCL17 effectively reversed these LPS-driven alterations. It significantly attenuated the LPS-induced expression of M1 markers (CD16, CD32, iNOS) and promoted a shift towards the M2 phenotype, indicated by the increased expression of CD206 and Arg-1, although IL-10 levels remained unchanged (Figure 5A-F).

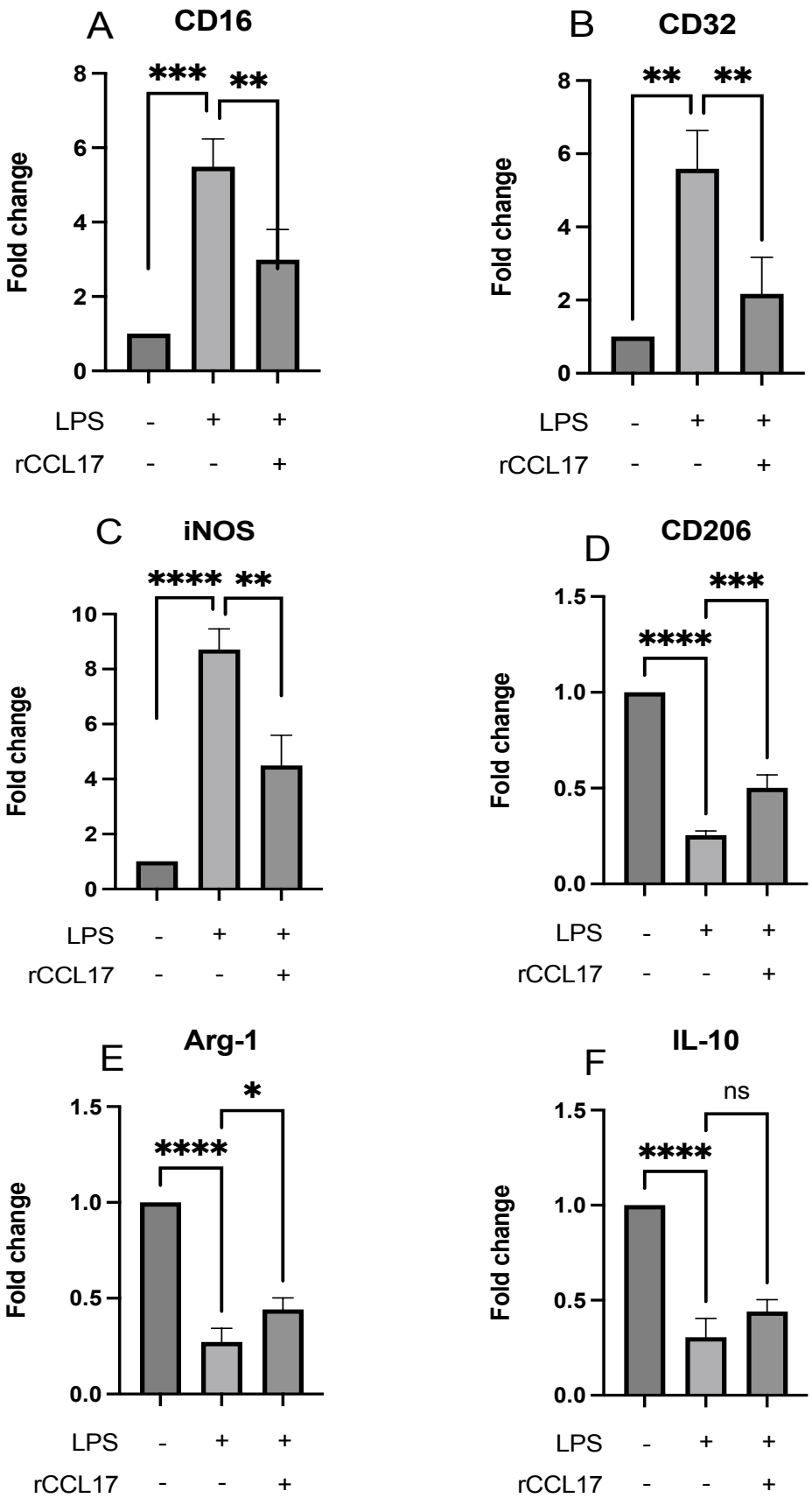

Figure 5. rCCL17 attenuates LPS-induced microglial polarization. RT-qPCR analysis of (A-C) M1 and (D-F) M2 phenotype marker expression in primary microglia across Control,

LPS, and LPS + rCCL17 (150 ng/mL) treatment groups (n=4). ns, not significant; *p < 0.05, **p < 0.01, ***p < 0.001, ****p < 0.0001, ANOVA.

3.3. rCCL17 enhances primary neuron viability under OGD/R conditions

To define the optimal OGD/R conditions for evaluating rCCL17's influence on neuronal viability, we first investigated the hypoxia duration (2-8 h) in primary cortical cultures. A 4-hour OGD followed by 24 h reoxygenation was found to produce a consistent 50% reduction in cell survival (Figure 6). This paradigm was therefore adopted for further investigations into rCCL17-mediated neuroprotection.

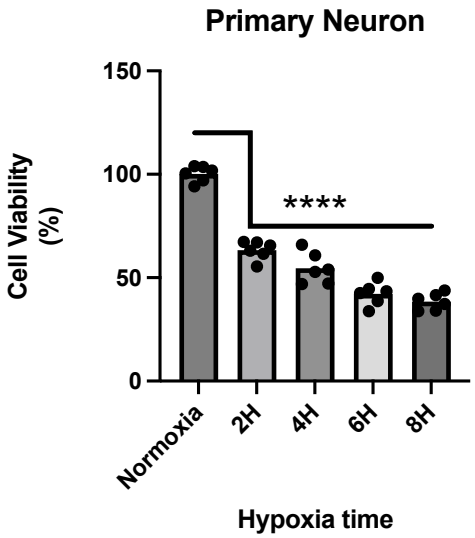

Figure 6. MTT assay for the viability of primary neurons under different durations of hypoxia. Each group included six technical replicates. ****p < 0.0001, ANOVA.

To address whether rCCL17 confers protection against OGD-triggered neuronal damage, we examined its effects across a concentration gradient (50, 100, and 150 ng/mL) in primary neuronal cultures subjected to hypoxia. The treatment with rCCL17 seemed to have a concentration dependent protective effect and cell viability was increased compared to the 0 ng/mL control group. Treatment with 50 ng/mL rCCL17 did not significantly enhance cell viability. In contrast, both 100 and 150 ng/mL concentrations markedly increased neuronal survival compared to the untreated OGD/R controls (Figure 7).

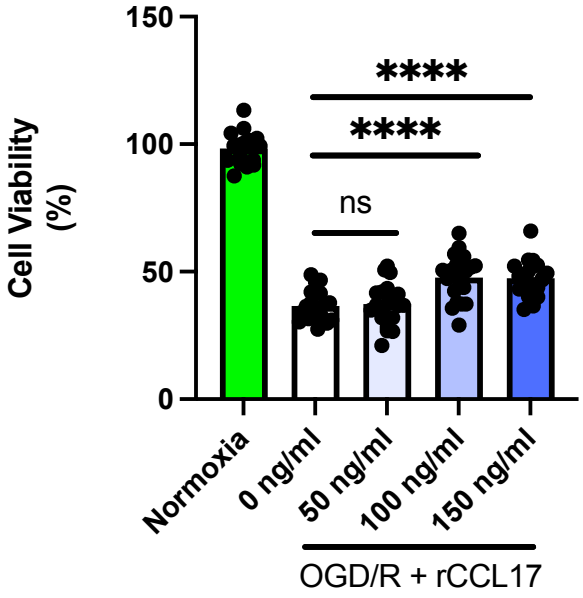

Figure 7. Cell viability of primary neurons under normoxic and OGD conditions treated with varying concentrations of rCCL17, as assessed by the MTT assay. All data points are derived from three separate experimental replications (n = 3), each performed with six to eight parallel replicates. ns, not significant; ****p < 0.0001, ANOVA.

3.4. rCCL17-pretreated microglia protect neurons under OGD/R conditions

We next aimed to assess the effect of rCCL17-preconditioned microglia on OGD/R-challenged primary neurons. For this purpose, a microglia-neuron co-culture model was implemented. All the groups exposed to OGD/R showed a reduced cell viability (Figure 8). Neurons co-cultured with microglia displayed an increased cell viability, however, the increase was only significant in the rCCL17-pretreated group.

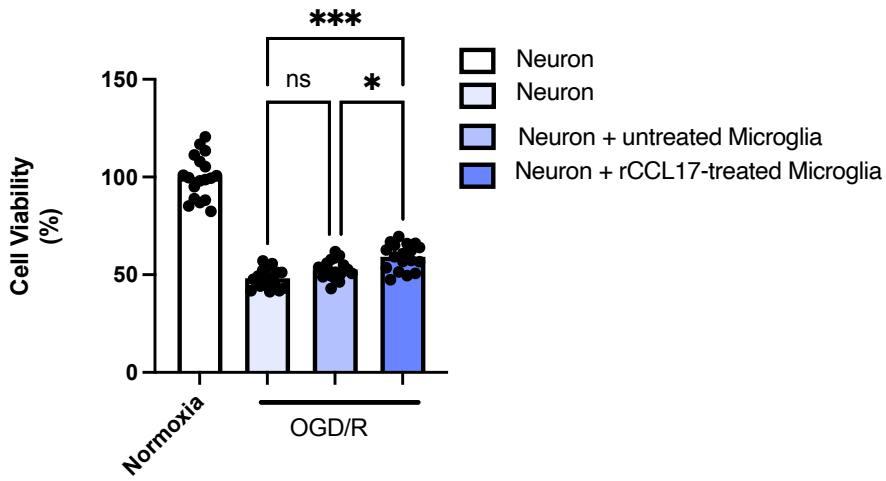

Figure 8. The effect of rCCL17-pretreated microglia on the viability of primary neurons. Data represent pooled results from three independent experiments (n = 3), each performed with six parallel replicates. ns, not significant; *p < 0.05, ***p < 0.001, ANOVA.

As apoptotic cell death is the primary pathological feature in the ischemic penumbra, we were also interested in the role of microglia on neuronal apoptosis. The activation of Caspase-3 plays a central role in executing neuronal apoptosis after ischemic brain injury. Therefore, we examined the caspase-3 protein levels in our co-culture model. We observed elevated caspase-3 expression in all OGD/R-exposed groups relative to the normoxic control (Figure 9). The neuron only group showed the biggest increase in expression, while co-culturing with microglia led to a reduced expression of caspase-3 compared to them. However, the reduction was only significant in the group with the rCCL17-pretreatd microglia. A marked decrease in cleaved caspase-3 was observed in neurons co-cultured with rCCL17-primed microglia relative to the OGD/R (neuron) control under the same OGD/R conditions (Figure 9).

A

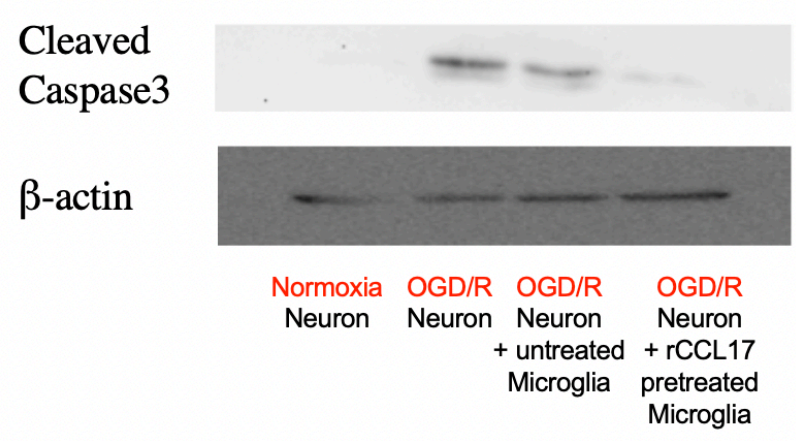

B

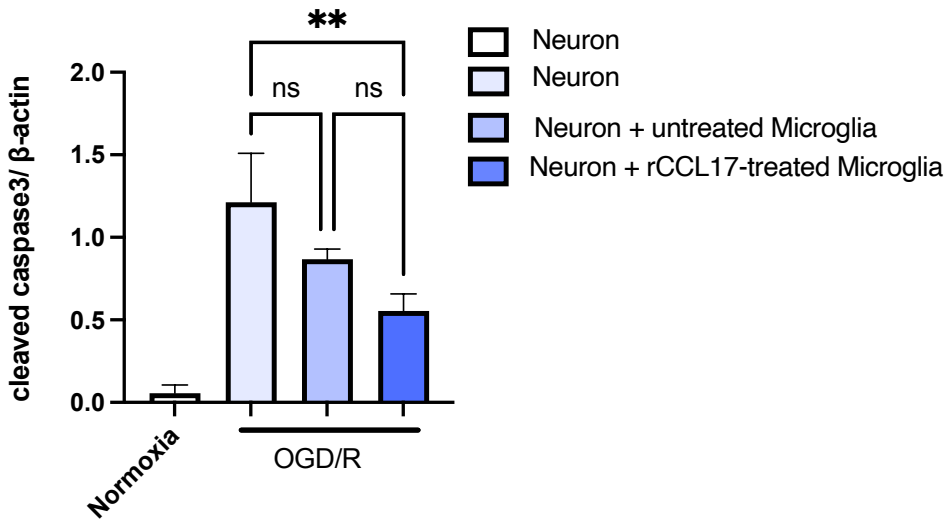

Figure 9. The effect of rCCL17-pretreated microglia on neuronal apoptosis under OGD/R conditions. (A and B) Cleaved Caspase-3 levels were assessed by Western blot across three independent replicates (n=3). ns, no significant. ** $p < 0.01$, ANOVA.

4. DISCUSSION

4.1. Characterization of primary microglia

We aimed to elucidate how specific stimuli affect the physiology of microglial cells in vitro. Compared to animal models, in vitro approaches offer the advantage of eliminating confounding factors, making it easier to observe and analyze the effects of individual factors on cellular models. Therefore, the primary task is to isolate highly pure and highly viable primary microglia. Below, we will discuss some key details.

Regarding the selection of experimental materials, data from earlier studies suggest that the age of mice strongly influences the success of primary cell isolation, particularly in terms of resulting purity and cell viability (Woolf et al. 2021). Cells isolated from the cortices of younger mice were more numerous and exhibited stronger adhesion capacity. The evidence shows that cells from neonate, or day-old fetal mice have a better survival rate (Daniele, Edwards, and Maguire-Zeiss 2014; Lian, Roy, and Zheng 2016). Due to institutional animal facility and breeder management policies, we rarely had access to P0 mice. Primary cells were therefore mainly isolated from P1–P3 pups. This limitation, however, did not substantially impact cell yield or purity.

The highest density of microglia required for this study existed in the gray matter. Therefore, it is essential to keep as much of the cerebral cortex as possible while minimizing the inclusion of the brainstem and cerebellum. Removing excess brainstem and cerebellar tissue prior to cell isolation helps eliminate interference from non-relevant tissues, thereby maximizing the purity of the target cells (Lian, Roy, and Zheng 2016). Additionally, the meningeal tissue and associated blood vessels on the surface of the brain should be removed carefully to prevent contamination from vascular endothelial cells, pia mater cells, and fibroblasts (Lian, Roy, and Zheng 2016).

The preparation of the single-cell suspension is crucial. This step differs slightly based on different protocols used, such as mechanical dissociation, papain digestion, or low-concentration trypsin digestion (Saura, Tusell, and Serratosa 2003; Daniele, Edwards, and

Maguire-Zeiss 2014; Jose et al. 2015; Lian, Roy, and Zheng 2016; Lin et al. 2017; Du et al. 2021; Woolf et al. 2021). We have tried all these methods and there is no clear difference in their effectiveness.

To collect microglia, the means of separation are roughly divided into two major categories: enzymatic digestion and mechanical shaking. The enzymatic digestion method consists in carrying out an enzymatic digestion with a mixture of trypsin-DMEM in a certain proportion (Saura, Tusell, and Serratosa 2003). During the incubation period, the detachment of the astrocyte layer should be monitored regularly. Eventually, when detachment is complete, the microglia will adhere to the bottom of the culture flasks. After digestion, we simply remove the supernatant to obtain highly purified microglial cells. The separation of the astrocytic layer is because of the calcium ions in the trypsin, and this phenomenon disappeared without calcium. Mechanical dissociation method is also similar. In general, there are two major ways. One method is to sharply tap the flask against a hard surface and collect the detached cells from the culture medium. The other method is placing the flasks in an incubation shaker, setting the appropriate speed and duration, to detach the cells (Du et al. 2021). We successfully obtained highly viable and purified microglial cells using the first method.

To verify whether the isolated cells were microglia, we performed immunofluorescence staining for two well-established microglial markers, CD206 and Iba-1. CD206 is a cell surface receptor used to identify microglia exhibiting the anti-inflammatory M2 phenotype (Cummings 2022). This receptor interacts with carbohydrate structures such as mannose, playing a role in endocytosis and pathogen clearance. Iba-1 is a commonly used pan-microglial marker that labels both resting and activated microglia by binding to actin-regulating proteins involved in membrane ruffling and phagocytosis (Ahmed et al. 2007). The presence of these two markers in cultures proves that we have successfully isolated microglial cells.

Our study lays the foundation for the phenotypic changes of microglia under different conditions.

4.2. CCL17 diverts microglia polarization by suppressing M1 and promoting M2 repolarization under OGD/R conditions and LPS stimulation

CCL17 as a chemokine has been implicated for modulating the immune response and specifically recruiting Treg cell (Riezu-Boj et al. 2011; Feng et al. 2022; Carbo et al. 2021; Weber et al. 2011). For example, by activating CCR4 and interfering with CCL22-driven β-arrestin signaling, CCL17 limits regulatory T cell migration into injured myocardium—exacerbating inflammation, fibrosis, and adverse remodeling following cardiac injury (Feng et al. 2022). Besides, it has recently drawn attention as a neuroimmune mediator in hemorrhagic stroke. In both intracerebral hemorrhage (ICH) and subarachnoid hemorrhage (SAH) models, rCCL17 reduced inflammation and neuronal cell death via CCR4-dependent pathways to improve outcomes (Deng et al. 2021; Zhang et al. 2022). Furthermore, CCL17 is naturally produced by hippocampal CA1 neurons, where it influences the morphology of microglia and synapses. This suggests that CCL17 contributes to maintaining the homeostasis of the CNS (Fulle et al. 2018).

However, its role in microglial polarization under OGD/R conditions has been less explored. M2 microglia represent an anti-inflammatory and neuroprotective phenotype involved in tissue repair and resolution of inflammation following CNS injury (Cherry, Olschowka, and O'Banion 2014; Varin and Gordon 2009). Our results show that under OGD/R stress, 150 ng/ml rCCL17 encouraged microglia to adopt the M2 state. To investigate if CCL17 has an anti-inflammatory effect, we tested its effect after LPS stimulation. As a potent immunostimulator, Lipopolysaccharide (LPS) is commonly used to cause a powerful pro-inflammatory response in microglia through activating TLR4 pathway (An et al. 2020). This model is mainly used to simulate neuroinflammation, which will promote macrophages or microglia to secrete large amounts of inflammatory factors, thereby transforming microglia into M1 phenotype (Plociennikowska et al. 2015). rCCL17 (150 ng/ml) rebalanced microglial M1/M2 polarization toward an anti-inflammatory state, this was consistent with rCCL17's effect under OGD/R stress. Together, these findings reveal that the therapeutic potential of CCL17 extends to broader

neuroinflammatory contexts. Given that M2 microglia are associated with neuroprotection and tissue repair (Orihuela, McPherson, and Harry 2016; Xue et al. 2021), the ability of CCL17 to modulate this balance may have therapeutic implications for ischemic stroke and neuroinflammatory diseases.

Another point to consider is that CCL17 may act through its receptor. CCR4 is known to bind to CCL17 specifically. How CCL17 induces the M1-to-M2 shift, and whether this involves direct action through microglial CCR4, remains unclear. Pharmacologically inactivating or genetically knocking out CCR4 on microglia might give us hints about how CCL17 works. Moreover, recently it was shown that CCL17 can also activate cells via a non-canonical pathway, namely that via CCR8 (Doring et al. 2024). Whether CCL17 regulates microglial polarization through this receptor deserves further investigation.

In addition, our results show a rCCL17 dose-dependent decrease in CD16 expression. At 100 ng/ml, rCCL17 reduced CD16 mRNA levels by approximately 25% compared to the LPS-only group ($p < 0.05$), but at 150 ng/ml, expression levels were reduced by half ($p < 0.0001$). Future studies could investigate whether the effect is more pronounced at higher doses.

To sum up, this work establishes a novel role for CCL17 in regulating microglial polarization under both ischemic and inflammatory conditions. CCL17 suppresses M1 markers as well as promoting M2 markers, this shows CCL17 can temper neuroinflammation.

4.3. CCL17 enhances primary neuron viability under OGD/R conditions

Neuronal loss is a prominent feature of ischemic stroke and a key cause of chronic neurological deficits (Dirnagl, Iadecola, and Moskowitz 1999). Ischemia quickly ruins the energy metabolism of neurons, leading to excitotoxicity, oxidative stress, then cell death (Brouns and De Deyn 2009). This everlasting loss, especially in key zones such as

the movement cortex or hippocampus, leads straight to actual malfunctions like movement weakness and brainpower diminishment (Lo, Dalkara, and Moskowitz 2003). In addition, dying neurons emit damage-associated molecular patterns which activate glia cells, intensifying neuroinflammation and secondary harm (Chamorro et al. 2016). Since the brain's regenerative capabilities are quite poor, neuroprotection, or the preservation of neurons, is one of the primary goals for stroke therapy.

We chose primary neurons over standard neuronal cell lines to approximate the physiological environment of the CNS more closely. Compared with immortalized cell lines like SH-SY5Y or PC12, primary neurons can maintain the complex morphology, electrophysiology and synaptic connections of mature neurons, which makes them a better model of in vivo neuronal functions (Brewer 1997; Kaech and Banker 2006). More importantly, these primary neurons have more accurate expressions of genes and proteins (Dehmelt and Halpain 2005; Sahu et al. 2019). The use of primary neurons is a more biologically relevant system to study neuronal injury and neuroprotection in vitro.

In this study, we isolated cortical neurons from E16.5 mouse embryos. Following dissection, meninges were carefully removed under a microscope to avoid contamination from non-neuronal cells. Then the cortical tissue was enzymatically dissociated with papain, a gentle protease that keeps the neuronal survival and morphology intact during isolation (Kaech and Banker 2006; Cramer and Tyagarajan 2024). We seeded our dissociated cells on cell culture plates coated with PDL to let them adhere and start growing their neurites. We chose Neurobasal medium for these cultures because this is a serum free medium formulated to support long-term neuronal survival and limit glial proliferation (Cramer and Tyagarajan 2024). Our workflow allowed us to obtain high-quality primary neurons for the following experiments.

In our MTT assay we found that after 4 h of OGD primary cortical neurons suffered significant injury, thus making it a good time point for the next experiments. This conforms to earlier evidence showing that as few as 90 min-6 h of OGD may be sufficient

to induce detectable damage in neural cells in primary culture(Chen et al. 2022; Wang et al. 2013; Pan et al. 2024). Slight variations in injury onset may be related to brain area, animal, or assay sensitivity. In conclusion, our studies demonstrate that 4 h of OGD represents a reliable and reproducible condition of neuronal injury in vitro.

At last, we study the influence of rCCL17 on the survival of primary neurons under hypoxia. The results indicated that rCCL17 at concentrations of 100 ng/ml and 150 ng/ml significantly increased neuronal survival after OGD, whereas 50 ng/ml did not exhibit a significant protective effect, suggesting a threshold concentration for neuroprotection. Consistent with prior work, chemokines can mediate neuroprotection by modulating inflammation, promoting neuronal survival, or promoting repair in a pathological environment (Deng et al. 2021; Zhan et al. 2024; Zhang et al. 2024), and more studies should be done to understand the mechanism. And CCL17's neuroprotective mechanism may be via different mechanisms. It may directly stimulate CCR4 receptors on neurons, activating survival-supporting signaling pathways like PI3K/Akt or ERK1/2 (Liu et al. 2025), known for its role in increasing neuronal survival post-ICH (Deng et al. 2021).

Furthermore, CCL17 have been identified to possess dual roles of disease. For instance, It has been show that CCL17 worsens myocardial injury since it reduces the cardioprotective regulatory T cell recruitment, which makes inflammation get fiercer inside the cardiac tissue (Feng et al. 2022). Similarly, in a murine model of colitis, CCL17 contributes to intestinal inflammation and antagonizes the protection offered by regulatory T cells (Heiseke et al. 2012). In contrast, a phase I trial of the anti-CCL17 antibody GSK3858279 showed a good safety profile and potential analgesic effects in healthy volunteers and patients with osteoarthritis (Nijjar et al. 2025). However, in our results there is a protection against hypoxic neuronal injury. It may be due to different conditions, cell types, or the temporal dynamics of CCL17 action.

4.4. CCL17-pretreated microglia protect neurons under OGD/R conditions

We studied the protective role of rCCL17-pretreated microglia on neurons subjected to OGD/R. Our MTT results showed that co-culturing of neurons with microglia following pretreatment with rCCL17 (150 ng/ml, 24 h) led to better neuronal survival in comparison to neuron cultured alone. It was interesting to find out that microglia not pretreated with rCCL17 did not improve neuron survival suggesting that CCL17 stimulation is necessary for neuroprotection. This indicates that CCL17 modulates microglia by turning them from M1 to M2 to lessen ischemic injury.

One potential mechanism underlying this effect is the regulation of apoptosis. Apoptosis is a major form of neuronal cell death in the ischemic penumbra following stroke (Radak et al. 2017). Among the apoptotic pathways, caspase-3 activation is a key event in neuronal apoptosis after ischemic injury (Nakka et al. 2008). We detected significantly elevated levels of cleaved caspase-3 in neurons co-cultured with rCCL17-pretreated microglia via western blot analysis, suggesting that CCL17 may exert an anti-apoptotic effect. These results align with previous reports suggesting that CCL17 plays a regulatory role in microglial activation, thereby facilitating neuronal survival in models of SAH and ICH (Deng et al. 2021; Zhang et al. 2022).

But it is important to acknowledge the limitations of using cleaved caspase-3 as the sole marker for apoptosis. Cleaved caspase-3 is a well-established executioner caspase in the apoptotic cascade, and its activation is considered a hallmark of apoptosis (Gong et al. 2019). However, apoptosis is a tightly controlled form of programmed cell death that involves a series of biochemical and morphological changes such as activation of signaling cascade, mitochondrial dysfunction, DNA fragmentation, and membrane blebbing (Arandjelovic and Ravichandran 2015; Gong et al. 2019; Kalkavan and Green 2018; Tait et al. 2010; Riley et al. 2018). Therefore, cleaved caspase-3 alone might not give a complete picture of complexity or extent of apoptotic cell death. In addition to this, future tests are needed in the future, for example TUNEL staining, Annexin V/PI flow cytometry, or testing on mitochondrial dysfunctions, to assess how well neurons can

survive. Activation of caspase-3 does not necessarily mean that cells will undergo apoptosis (Eskandari and Eaves 2022). Sublethal caspase-3 activation has been shown to affect non-apoptotic cellular functions such as cell proliferation via proteolytic cleavage of a variety of protein substrates (Li et al. 2010; Yosefzon et al. 2018). Take the mouse epidermis as an example: it is critical for normal epidermal cell regeneration and for maintaining sebaceous gland without involving apoptosis (Yosefzon et al. 2018). These findings point out that there might also be caspase-3 activation even if it doesn't lead to normal kinds of cell deaths. Also, caspase-3 by itself shouldn't be seen as sure sign to predict the fate of a cell. Furthermore, there could be caspase-independent forms of cell death, such as necroptosis or autophagy-associated cell death, which have little correlation with caspase-3 activation.

In addition, evidence indicates that ferroptosis contributes significantly to the pathogenesis of ischemic stroke, especially in the penumbra area, which is characterized by a high degree of oxidative stress and iron accumulation (Alim et al. 2019; Wang et al. 2023). Nuclear factor erythroid 2-related factor 2 (Nrf2) is a master regulator of antioxidant defense and cellular redox homeostasis (Li et al. 2024; Wang et al. 2024; Xiao et al. 2024; Zi et al. 2023). Intriguingly, a latest investigation in the context of ICH demonstrated that the CCL17/CCR4 signaling axis can enhance Nrf2 expression (Deng et al. 2020). Given that oxidative stress and ferroptosis are both central drivers to OGD/R induced neuronal injury, it is reasonable to believe that CCL17 could exert neuroprotection in more ways not only through the mechanism described above but also by inhibiting ferroptosis via Nrf2 induction. Although we haven't done any experiments on ferroptosis-related markers such as lipid peroxidation levels or GPX4 expression, this way of cell death is worth a look. Future studies could include the use of ferroptosis specific inhibitors (e.g., ferrostatin-1), and evaluation of downstream Nrf2 targets to determine to what extent the CCL17/CCR4-Nrf2 axis influences neuronal survival in the OGD/R model.

4.5. Limitations

This study has some limitations. Firstly, although our study focused on the role of microglial CCR4 in mediating the neuroprotective effects of CCL17, CCR4 expression is not limited to microglia (Fulle et al. 2018; Zhang et al. 2022; Deng et al. 2021). However, the potential contributions of these cell types were not examined in this study. Future studies should investigate the cell-type-specific roles of CCR4 to better delineate the mechanisms underlying CCL17-mediated neuroprotection. Second, neuronal apoptosis was assessed solely by cleaved caspase-3, which is insufficient to show the full picture of apoptotic pathways. Additional assays are needed to validate the anti-apoptotic effect. Third, although we speculated on the involvement of ferroptosis and the CCL17/CCR4-Nrf2 axis, no direct ferroptosis markers were examined. Finally, all the experiments conducted were in vitro, so in vivo experiments are needed to give more evidence in the future.

5. SUMMARY

This study finds that CCL17 has various neuroprotective functions under ischemia and inflammation. CCL17 can inhibit M1 microglial polarization and induce a shift toward M2 polarization under both OGD/R and LPS challenge, and this results in the establishment of an anti-inflammatory environment. Moreover, CCL17 itself has a direct promotion on the survival of primary neurons under hypoxia, and it's indirectly validated via the cocultures, where CCL17-pretreated microglia boost the neuronal cell number and reduce neuronal cell apoptosis. Together, these findings establish a significant role for CCL17 in altering neuroinflammation and facilitating neuronal survival in ischemic disease, underscoring its therapeutic promise for ischemic stroke and its neurodegenerative sequelae.

ABSTRACT

Ischemic stroke is a leading cause of death and disability worldwide, characterized by complex neuroinflammatory processes. Microglia serve as the innate immune cells within the central nervous system and are central mediators of neuroinflammatory responses. We investigated whether recombinant CCL17 (rCCL17) could influence microglial polarization and exert neuroprotective effects under OGD/R-induced injury conditions. Using brain tissue from neonatal mice, primary microglia were obtained and validated through morphological examination and immunofluorescence detection of IBA-1 and CD206. MTT assays revealed that microglial viability decreased significantly following prolonged hypoxia, establishing a 4-hour OGD with 24-hour reoxygenation as the experimental paradigm. Exposure to OGD/R conditions induced a marked increase in M1-associated genes—CD16, CD32, and iNOS—in microglia, whereas M2 markers like CD206, Arg-1, and IL-10 exhibited minimal upregulation. Notably, rCCL17 treatment at 150 ng/mL mitigated this pro-inflammatory response, facilitating a shift toward the M2 phenotype with elevated expression of associated markers. Furthermore, LPS stimulation led to increased M1 marker expression and a reduction in M2 markers, an effect that was reversed by rCCL17 treatment, except for IL-10. To assess the impact of rCCL17 on neuronal survival, primary neurons were subjected to OGD/R, revealing significant cell death after 4 h of hypoxia. rCCL17 at 100 ng/mL and 150 ng/mL significantly improved neuronal viability. When neurons were co-cultured with rCCL17-pretreated microglia, neuronal viability was significantly improved. Western blot analysis further confirmed that rCCL17-pretreated microglia reduced cleaved caspase-3 levels in neurons, indicating an anti-apoptotic effect. These results point to CCL17 as a modulator of microglial polarization, dampening M1-related responses and favoring M2-associated functions, thereby exerting neuroprotective effects under ischemic conditions. Evidence from this work suggests that CCL17 could be developed as an effective treatment for ischemic stroke.

Zusammenfassung

Der ischämische Schlaganfall ist weltweit eine der häufigsten Ursachen für Tod und Behinderung und ist durch komplexe neuroinflammatorische Prozesse gekennzeichnet. Mikrogliazellen dienen als angeborene Immunzellen des zentralen Nervensystems und sind zentrale Vermittler neuroinflammatorischer Reaktionen. In der vorliegenden Arbeit wurde untersucht, ob rekombinantes CCL17 (rCCL17) die Polarisation von Mikrogliazellen beeinflussen und unter OGD/R-induzierten Schädigungsbedingungen neuroprotektive Effekte entfalten kann. Aus Gehirngewebe neugeborener Mäuse wurden primäre Mikrogliazellen isoliert und mittels morphologischer Untersuchung sowie Immunfluoreszenzfärbung für IBA-1 und CD206 validiert. MTT-Assays ergaben, dass die Viabilität der Mikrogliazellen nach längerer Hypoxie signifikant abnahm, sodass ein 4-stündiges OGD mit anschließender 24-stündiger Reoxygenierung als experimentelles Paradigma etabliert wurde. Die Exposition gegenüber OGD/R-Bedingungen induzierte eine deutliche Hochregulation von M1-assoziierten Genen (CD16, CD32 und iNOS) in Mikrogliazellen, wohingegen M2-Marker wie CD206, Arg-1 und IL-10 kaum hochreguliert wurden. Bemerkenswerterweise milderte eine Behandlung mit rCCL17 in einer Konzentration von 150 ng/mL diese proinflammatorische Antwort, indem sie eine Verschiebung hin zum M2-Phänotyp förderte, was sich in einer erhöhten Expression der assoziierten Marker widerspiegelte. Darüber hinaus induzierte eine Stimulation mit LPS eine gesteigerte Expression von M1-Markern und eine Reduktion von M2-Markern – ein Effekt, der durch rCCL17, mit Ausnahme von IL-10, rückgängig gemacht wurde. Um den Einfluss von rCCL17 auf das Überleben von Neuronen zu evaluieren, wurden primäre Neuronen OGD/R-Bedingungen ausgesetzt, was einen signifikanten Zelltod zur Folge hatte nach 4 Stunden Hypoxie. rCCL17 in Konzentrationen von 100 ng/mL und 150 ng/mL verbesserte die neuronale Viabilität signifikant. Wurden Neuronen mit rCCL17-vorbehandelten Mikrogliazellen ko-kultiviert, ergab sich ebenfalls eine signifikant gesteigerte neuronale Viabilität. Western-Blot-Analysen bestätigten weiterhin, dass rCCL17-vorbehandelte Mikrogliazellen die Menge an gespaltenem Caspase-3 in Neuronen verringerten, was auf einen antiapoptotischen Effekt hinweist. Diese

Ergebnisse legen nahe, dass CCL17 als Modulator der Mikroglia-Polarisation wirkt, indem es M1-assoziierte Reaktionen abschwächt und M2-assoziierte Funktionen fördert und somit unter ischämischen Bedingungen neuroprotektive Effekte entfaltet. Die vorliegenden Befunde legen nahe, dass CCL17 als potenziell wirksame Therapieoption für den ischämischen Schlaganfall entwickelt werden könnte.

ABBREVIATION

3-MA	3-Methyladenine
APS	Ammonium persulfate
BBB	Blood-brain barrier
BSA	Bovine Serum Albumin
BSS0	Glucose-free balanced salt solution
CCR4	CC chemokine receptor 4
CNS	Central nervous system
COX-2	Cyclooxygenase-2
DAPI	4',6-Diamidino-2-phenylindol dihydrochloride
DD	Death domain
DISC	Death-inducing signaling complex
DMSO	Dimethyl sulfoxide
DPBS	Dulbecco's phosphate buffered saline
DRs	Death receptors
ECL	Enhanced chemoluminescence
FADD	Fas-associated DD
FASL	Fas ligand
FBS	Fetal bovine serum
HBSS	Hanks' Balanced Salt Solution
IFN	Interferon
LPS	Lipopolysaccharide
MMPs	Matrix metalloproteinases
MTT	3-(4,5-Dimethyl-2-thiazolyl)-2,5-diphenyl-2H-tetrazolium Bromide
NF-κB	Nuclear factor kappa-light-chain-enhancer of activated B cells
Nrf-2	Nuclear factor erythroid 2-related factor 2
OGD	Oxygen-glucose deprivation

PARP	Poly (ADP-ribose) polymerase
PCR	Polymerase Chain Reaction
PDA	Poly-D-lysine
PFA	Paraformaldehyde
R	Reoxygenation
RPM	Revolutions Per Minute
RT	Room temperature
SD	Standard deviation
SDS	Sodium dodecyl sulfate
SMAC	Second mitochondria-derived activator of caspases
TEMED	Tetramethyl ethylenediamine
TLR4	Toll-like receptor 4
TNF	Tumor necrosis factor
TNF-α	Tumor necrosis factor-α
TRADD	TNF receptor-associated DD
Tregs	Regulatory T cells
Tris	Trishydroxymethyl aminomethan
ICH	Intracerebral hemorrhage
qRT-PCR	Quantitative real-time PCR
SAH	Subarachnoid hemorrhage
tPA	Tissue plasminogen activator

REFERENCE

Ahmed, Z., G. Shaw, V. P. Sharma, C. Yang, E. McGowan, and D. W. Dickson. 2007. 'Actin-binding proteins coronin-1a and IBA-1 are effective microglial markers for immunohistochemistry', *J Histochem Cytochem*, 55: 687-700.

Al Mamun, A., A. Chauhan, S. Qi, C. Ngwa, Y. Xu, R. Sharmeen, A. L. Hazen, J. Li, J. A. Aronowski, L. D. McCullough, and F. Liu. 2020. 'Microglial IRF5-IRF4 regulatory axis regulates neuroinflammation after cerebral ischemia and impacts stroke outcomes', *Proc Natl Acad Sci U S A*, 117: 1742-52.

Alim, I., J. T. Caulfield, Y. Chen, V. Swarup, D. H. Geschwind, E. Ivanova, J. Seravalli, Y. Ai, L. H. Sansing, E. J. Ste Marie, R. J. Hondal, S. Mukherjee, J. W. Cave, B. T. Sagdullaev, S. S. Karuppagounder, and R. R. Ratan. 2019. 'Selenium Drives a Transcriptional Adaptive Program to Block Ferroptosis and Treat Stroke', *Cell*, 177: 1262-79 e25.

An, J., B. Chen, X. Kang, R. Zhang, Y. Guo, J. Zhao, and H. Yang. 2020. 'Neuroprotective effects of natural compounds on LPS-induced inflammatory responses in microglia', *Am J Transl Res*, 12: 2353-78.

Anderson, C. A., P. Patel, J. M. Viney, R. M. Phillips, R. Solari, and J. E. Pease. 2020. 'A degradatory fate for CCR4 suggests a primary role in Th2 inflammation', *J Leukoc Biol*, 107: 455-66.

Arandjelovic, S., and K. S. Ravichandran. 2015. 'Phagocytosis of apoptotic cells in homeostasis', *Nat Immunol*, 16: 907-17.

Ashkenazi, A. 2002. 'Targeting death and decoy receptors of the tumour-necrosis factor superfamily', *Nat Rev Cancer*, 2: 420-30.

Barone, F. C., and G. Z. Feuerstein. 1999. 'Inflammatory mediators and stroke: new opportunities for novel therapeutics', *J Cereb Blood Flow Metab*, 19: 819-34.

Basic Kes, V., A. M. Simundic, N. Nikolac, E. Topic, and V. Demarin. 2008. 'Pro-inflammatory and anti-inflammatory cytokines in acute ischemic stroke and their relation to early neurological deficit and stroke outcome', *Clin Biochem*, 41: 1330-4.

Berglund, R., A. O. Guerreiro-Cacais, M. Z. Adzemovic, M. Zeitelhofer, H. Lund, E. Ewing, S. Ruhrmann, E. Nutma, R. Parsa, M. Thessen-Hedreul, S. Amor, R. A. Harris, T. Olsson, and M. Jagodic. 2020. 'Microglial autophagy-associated phagocytosis is essential for recovery from neuroinflammation', *Sci Immunol*, 5.

Brewer, G. J. 1997. 'Isolation and culture of adult rat hippocampal neurons', *J Neurosci Methods*, 71: 143-55.

Broughton, B. R., D. C. Reutens, and C. G. Sobey. 2009. 'Apoptotic mechanisms after cerebral ischemia', *Stroke*, 40: e331-9.

Brouns, R., and P. P. De Deyn. 2009. 'The complexity of neurobiological processes in acute ischemic stroke', *Clin Neurol Neurosurg*, 111: 483-95.

Carbo, J. M., T. E. Leon, J. Font-Diaz, J. V. De la Rosa, A. Castrillo, F. R. Picard, D. Staudenraus, M. Huber, L. Cedo, J. C. Escola-Gil, L. Campos, L. Bakiri, E. F. Wagner, C. Caelles, T. Stratmann, J. A. Van Ginderachter, and A. F. Valledor. 2021. 'Pharmacologic Activation of LXR Alters the Expression Profile of Tumor-Associated Macrophages and the Abundance of Regulatory T Cells in the Tumor Microenvironment', *Cancer Res*, 81: 968-85.

Chamorro, A., U. Dirnagl, X. Urra, and A. M. Planas. 2016. 'Neuroprotection in acute stroke: targeting excitotoxicity, oxidative and nitrosative stress, and inflammation', *Lancet Neurol*, 15: 869-81.

Chang, A. L., J. Miska, D. A. Wainwright, M. Dey, C. V. Rivetta, D. Yu, D. Kanojia, K. C. Pituch, J. Qiao, P. Pytel, Y. Han, M. Wu, L. Zhang, C. M. Horbinski, A. U. Ahmed, and M. S. Lesniak. 2016. 'CCL2 Produced by the Glioma Microenvironment Is Essential for the Recruitment of Regulatory T Cells and Myeloid-Derived Suppressor Cells', *Cancer Res*, 76: 5671-82.

Chen, H., G. Tang, J. Yu, and R. Yu. 2022. 'Neuroprotective Effects of Curcumin against Oxygen-Glucose Deprivation/Reoxygenation-Induced Injury in Cultured Primary Rat Astrocyte by Improving Mitochondrial Function and Regulating the ERK Signaling Pathway', *Evid Based Complement Alternat Med*, 2022: 1731701.

Cherry, J. D., J. A. Olschowka, and M. K. O'Banion. 2014. 'Neuroinflammation and M2 microglia: the good, the bad, and the inflamed', *J Neuroinflammation*, 11: 98.

Chia, N. H., J. M. Leyden, J. Newbury, J. Jannes, and T. J. Kleinig. 2016. 'Determining the Number of Ischemic Strokes Potentially Eligible for Endovascular Thrombectomy: A Population-Based Study', *Stroke*, 47: 1377-80.

Collaborators, G. B. D. Stroke. 2019. 'Global, regional, and national burden of stroke, 1990-2016: a systematic analysis for the Global Burden of Disease Study 2016', *Lancet Neurol*, 18: 439-58.

Cramer, S. C. 2008. 'Repairing the human brain after stroke. II. Restorative therapies', *Ann Neurol*, 63: 549-60.

Cramer, T. M. L., and S. K. Tyagarajan. 2024. 'Protocol for the culturing of primary hippocampal mouse neurons for functional in vitro studies', *STAR Protoc*, 5: 102991.

Cummings, R. D. 2022. 'The mannose receptor ligands and the macrophage glycome', *Curr Opin Struct Biol*, 75: 102394.

Daniele, S. G., A. A. Edwards, and K. A. Maguire-Zeiss. 2014. 'Isolation of cortical microglia with preserved immunophenotype and functionality from murine neonates', *J Vis Exp*: e51005.

Dehmelt, L., and S. Halpain. 2005. 'The MAP2/Tau family of microtubule-associated proteins', *Genome Biol*, 6: 204.

Deng, S., P. Jin, P. Sherchan, S. Liu, Y. Cui, L. Huang, J. H. Zhang, Y. Gong, and J. Tang. 2021. 'Recombinant CCL17-dependent CCR4 activation alleviates neuroinflammation and neuronal apoptosis through the PI3K/AKT/Foxo1 signaling pathway after ICH in mice', *J Neuroinflammation*, 18: 62.

Deng, S., P. Sherchan, P. Jin, L. Huang, Z. Travis, J. H. Zhang, Y. Gong, and J. Tang. 2020. 'Recombinant CCL17 Enhances Hematoma Resolution and Activation of CCR4/ERK/Nrf2/CD163 Signaling Pathway After Intracerebral Hemorrhage in Mice', *Neurotherapeutics*, 17: 1940-53.

Devanney, N. A., A. N. Stewart, and J. C. Gensel. 2020. 'Microglia and macrophage metabolism in CNS injury and disease: The role of immunometabolism in neurodegeneration and neurotrauma', *Exp Neurol*, 329: 113310.

Dirnagl, U. 2004. 'Inflammation in stroke: the good, the bad, and the unknown', *Ernst Schering Res Found Workshop*: 87-99.

Dirnagl, U., C. Iadecola, and M. A. Moskowitz. 1999. 'Pathobiology of ischaemic stroke: an integrated view', *Trends Neurosci*, 22: 391-7.

Donnan, G. A., M. Fisher, M. Macleod, and S. M. Davis. 2008. 'Stroke', *Lancet*, 371: 1612-23.

Doring, Y., E. P. C. van der Vorst, Y. Yan, C. Neideck, X. Blanchet, Y. Jansen, M. Kemmerich, S. Bayasgalan, L. J. F. Peters, M. Hristov, K. Bidzhekov, C. Yin, X. Zhang, J. Leberzammer, Y. Li, I. Park, M. Kral, K. Nitz, L. Parma, S. Gencer, A. Habenicht, A. Faussner, D. Teupser, C. Monaco, L. Holdt, R. T. A. Megens, D. Atzler, D. Santovito, P. von Hundelshausen, and C. Weber. 2024. 'Identification of a non-canonical chemokine-receptor pathway suppressing regulatory T cells to drive atherosclerosis', *Nat Cardiovasc Res*, 3: 221-42.

Du, S., S. Xiong, X. Du, T. F. Yuan, B. Peng, and Y. Rao. 2021. 'Primary Microglia Isolation from Postnatal Mouse Brains', *J Vis Exp*.

Emberson, J., K. R. Lees, P. Lyden, L. Blackwell, G. Albers, E. Bluhmki, T. Brott, G. Cohen, S. Davis, G. Donnan, J. Grotta, G. Howard, M. Kaste, M. Koga, R. von Kummer, M. Lansberg, R. I. Lindley, G. Murray, J. M. Olivot, M. Parsons, B. Tilley, D. Toni, K. Toyoda, N. Wahlgren, J. Wardlaw, W. Whiteley, G. J. del Zoppo, C. Baigent, P. Sandercock, W. Hacke, and Group Stroke Thrombolysis Trialists' Collaborative. 2014. 'Effect of treatment delay, age, and stroke severity on the effects of intravenous thrombolysis with alteplase for acute ischaemic stroke: a meta-analysis of individual patient data from randomised trials', *Lancet*, 384: 1929-35.

Endres, M., M. A. Moro, C. H. Nolte, C. Dames, M. S. Buckwalter, and A. Meisel. 2022. 'Immune Pathways in Etiology, Acute Phase, and Chronic Sequelae of Ischemic Stroke', *Circ Res*, 130: 1167-86.

Eskandari, E., and C. J. Eaves. 2022. 'Paradoxical roles of caspase-3 in regulating cell survival, proliferation, and tumorigenesis', *J Cell Biol*, 221.

Feng, G., G. Bajpai, P. Ma, A. Koenig, A. Bredemeyer, I. Lokshina, L. Lai, I. Forster, F. Leuschner, D. Kreisel, and K. J. Lavine. 2022. 'CCL17 Aggravates Myocardial Injury by Suppressing Recruitment of Regulatory T Cells', *Circulation*, 145: 765-82.

Ferrer, I. 2006. 'Apoptosis: future targets for neuroprotective strategies', *Cerebrovasc Dis*, 21 Suppl 2: 9-20.

Ferrer, I., B. Friguls, E. Dalfo, C. Justicia, and A. M. Planas. 2003. 'Caspase-dependent and caspase-independent signalling of apoptosis in the penumbra following middle cerebral artery occlusion in the adult rat', *Neuropathol Appl Neurobiol*, 29: 472-81.

Flynn, G., S. Maru, J. Loughlin, I. A. Romero, and D. Male. 2003. 'Regulation of chemokine receptor expression in human microglia and astrocytes', *J Neuroimmunol*, 136: 84-93.

Font, M. A., A. Arboix, and J. Krupinski. 2010. 'Angiogenesis, neurogenesis and neuroplasticity in ischemic stroke', *Curr Cardiol Rev*, 6: 238-44.

Fraser, A., and G. Evan. 1996. 'A license to kill', *Cell*, 85: 781-4.

Fricker, M., A. M. Tolkovsky, V. Borutaite, M. Coleman, and G. C. Brown. 2018. 'Neuronal Cell Death', *Physiol Rev*, 98: 813-80.

Fulle, L., N. Offermann, J. N. Hansen, B. Breithausen, A. B. Erazo, O. Schanz, L. Radau, F. Gondorf, K. Knopper, J. Alferink, Z. Abdullah, H. Neumann, H. Weighardt, C. Henneberger, A. Halle, and I. Forster. 2018. 'CCL17 exerts a neuroimmune modulatory function and is expressed in hippocampal neurons', *Glia*, 66: 2246-61.

Furlan, A. J. 2015. 'Endovascular therapy for stroke--it's about time', *N Engl J Med*, 372: 2347-9.

Garcia, J. H. 1984. 'Experimental ischemic stroke: a review', *Stroke*, 15: 5-14.

Ghobrial, I. M., T. E. Witzig, and A. A. Adjei. 2005. 'Targeting apoptosis pathways in cancer therapy', *CA Cancer J Clin*, 55: 178-94.

Golks, A., D. Brenner, I. Schmitz, C. Watzl, A. Krueger, P. H. Krammer, and I. N. Lavrik. 2006. 'The role of CAP3 in CD95 signaling: new insights into the mechanism of procaspase-8 activation', *Cell Death Differ*, 13: 489-98.

Gomez-Angelats, M., and J. A. Cidlowski. 2001. 'Protein kinase C regulates FADD recruitment and death-inducing signaling complex formation in Fas/CD95-induced apoptosis', *J Biol Chem*, 276: 44944-52.

Gong, Y. N., J. C. Crawford, B. L. Heckmann, and D. R. Green. 2019. 'To the edge of cell death and back', *FEBS J*, 286: 430-40.

Green, D. R., and T. A. Ferguson. 2001. 'The role of Fas ligand in immune privilege', *Nat Rev Mol Cell Biol*, 2: 917-24.

Green, T. R. F., and R. K. Rowe. 2024. 'Quantifying microglial morphology: an insight into function', *Clin Exp Immunol*, 216: 221-29.

Greter, M., I. Lelios, and A. L. Croxford. 2015. 'Microglia Versus Myeloid Cell Nomenclature during Brain Inflammation', *Front Immunol*, 6: 249.

Han, B., W. Jiang, P. Cui, K. Zheng, C. Dang, J. Wang, H. Li, L. Chen, R. Zhang, Q. M. Wang, Z. Ju, and J. Hao. 2021. 'Microglial PGC-1alpha protects against ischemic brain injury by suppressing neuroinflammation', *Genome Med*, 13: 47.

Hankey, G. J. 2017. 'Stroke', *Lancet*, 389: 641-54.

Haudek, S. B., G. E. Taffet, M. D. Schneider, and D. L. Mann. 2007. 'TNF provokes cardiomyocyte apoptosis and cardiac remodeling through activation of multiple cell death pathways', *J Clin Invest*, 117: 2692-701.

He, T., W. Li, Y. Song, Z. Li, Y. Tang, Z. Zhang, and G. Y. Yang. 2020. 'Sestrin2 regulates microglia polarization through mTOR-mediated autophagic flux to attenuate inflammation during experimental brain ischemia', *J Neuroinflammation*, 17: 329.

Heiseke, A. F., A. C. Faul, H. A. Lehr, I. Forster, R. M. Schmid, A. B. Krug, and W. Reindl. 2012. 'CCL17 promotes intestinal inflammation in mice and counteracts regulatory T cell-mediated protection from colitis', *Gastroenterology*, 142: 335-45.

Hinkle, J. L., and M. M. Guanci. 2007. 'Acute ischemic stroke review', *J Neurosci Nurs*, 39: 285-93, 310.

Hribljan, V., D. Lisjak, D. J. Petrovic, and D. Mitrecic. 2019. 'Necroptosis is one of the modalities of cell death accompanying ischemic brain stroke: from pathogenesis to therapeutic possibilities', *Croat Med J*, 60: 121-26.

Hughes, C. E., and R. J. B. Nibbs. 2018. 'A guide to chemokines and their receptors', *FEBS J*, 285: 2944-71.

Hwang, J., K. N. Son, C. W. Kim, J. Ko, D. S. Na, B. S. Kwon, Y. S. Gho, and J. Kim. 2005. 'Human CC chemokine CCL23, a ligand for CCR1, induces endothelial cell migration and promotes angiogenesis', *Cytokine*, 30: 254-63.

Iadecola, C., and J. Anrather. 2011. 'Stroke research at a crossroad: asking the brain for directions', *Nat Neurosci*, 14: 1363-8.

Imtiyaz, H. Z., Y. Zhang, and J. Zhang. 2005. 'Structural requirements for signal-induced target binding of FADD determined by functional reconstitution of FADD deficiency', *J Biol Chem*, 280: 31360-7.

Jayaraj, R. L., S. Azimullah, R. Beiram, F. Y. Jalal, and G. A. Rosenberg. 2019. 'Neuroinflammation: friend and foe for ischemic stroke', *J Neuroinflammation*, 16: 142.

Jia, J., L. Yang, Y. Chen, L. Zheng, Y. Chen, Y. Xu, and M. Zhang. 2021. 'The Role of Microglial Phagocytosis in Ischemic Stroke', *Front Immunol*, 12: 790201.

Jin, R., L. Liu, S. Zhang, A. Nanda, and G. Li. 2013. 'Role of inflammation and its mediators in acute ischemic stroke', *J Cardiovasc Transl Res*, 6: 834-51.

Jin, R., G. Yang, and G. Li. 2010. 'Inflammatory mechanisms in ischemic stroke: role of inflammatory cells', *J Leukoc Biol*, 87: 779-89.

Jose, S., S. W. Tan, C. K. Tong, and S. Vidyadaran. 2015. 'Isolation and characterization of primary microglia from post-natal murine brain tissues: a comparison of two methods', *Cell Biol Int*, 39: 1355-63.

Jost, P. J., S. Grabow, D. Gray, M. D. McKenzie, U. Nachbur, D. C. Huang, P. Bouillet, H. E. Thomas, C. Borner, J. Silke, A. Strasser, and T. Kaufmann. 2009. 'XIAP discriminates between type I and type II FAS-induced apoptosis', *Nature*, 460: 1035-9.

Jurcau, A., and A. Simion. 2021. 'Neuroinflammation in Cerebral Ischemia and Ischemia/Reperfusion Injuries: From Pathophysiology to Therapeutic Strategies', *Int J Mol Sci*, 23.

Kaech, S., and G. Banker. 2006. 'Culturing hippocampal neurons', *Nat Protoc*, 1: 2406-15.

Kalkavan, H., and D. R. Green. 2018. 'MOMP, cell suicide as a BCL-2 family business', *Cell Death Differ*, 25: 46-55.

Kim, S., and Y. Son. 2021. 'Astrocytes Stimulate Microglial Proliferation and M2 Polarization In Vitro through Crosstalk between Astrocytes and Microglia', *Int J Mol Sci*, 22.

Koh, S. H., and H. H. Park. 2017. 'Neurogenesis in Stroke Recovery', *Transl Stroke Res*, 8: 3-13.

Kufareva, I., C. L. Salanga, and T. M. Handel. 2015. 'Chemokine and chemokine receptor structure and interactions: implications for therapeutic strategies', *Immunol Cell Biol*, 93: 372-83.

Lavrik, I., A. Golks, and P. H. Krammer. 2005a. 'Death receptor signaling', *J Cell Sci*, 118: 265-7.

Lavrik, I. N., A. Golks, and P. H. Krammer. 2005b. 'Caspases: pharmacological manipulation of cell death', *J Clin Invest*, 115: 2665-72.

Li, F., Z. He, J. Shen, Q. Huang, W. Li, X. Liu, Y. He, F. Wolf, and C. Y. Li. 2010. 'Apoptotic caspases regulate induction of iPSCs from human fibroblasts', *Cell Stem Cell*, 7: 508-20.

Li, Y., X. Zhu, W. Xiong, Q. Zhao, Y. Zhou, Y. Guo, B. Liu, M. Li, Q. Chen, X. Jiang, Y. Qi, Q. Ye, and G. Deng. 2024. 'Brain-targeted ursolic acid nanoparticles for anti-ferroptosis therapy in subarachnoid hemorrhage', *J Nanobiotechnology*, 22: 641.

Lian, H., E. Roy, and H. Zheng. 2016. 'Protocol for Primary Microglial Culture Preparation', *Bio Protoc*, 6.

Lin, L., R. Desai, X. Wang, E. H. Lo, and C. Xing. 2017. 'Characteristics of primary rat microglia isolated from mixed cultures using two different methods', *J Neuroinflammation*, 14: 101.

Lindhout, I. A., T. E. Murray, C. M. Richards, and A. Klegeris. 2021. 'Potential neurotoxic activity of diverse molecules released by microglia', *Neurochem Int*, 148: 105117.

Liu, C., K. Zhang, H. Shen, X. Yao, Q. Sun, and G. Chen. 2018. 'Necroptosis: A novel manner of cell death, associated with stroke (Review)', *Int J Mol Med*, 41: 624-30.

Liu, L. R., J. C. Liu, J. S. Bao, Q. Q. Bai, and G. Q. Wang. 2020. 'Interaction of Microglia and Astrocytes in the Neurovascular Unit', *Front Immunol*, 11: 1024.

Liu, T., X. Li, X. Zhou, W. Chen, A. Wen, M. Liu, and Y. Ding. 2025. 'PI3K/AKT signaling and neuroprotection in ischemic stroke: molecular mechanisms and therapeutic perspectives', *Neural Regen Res*, 20: 2758-75.

Lo, E. H. 2008. 'A new penumbra: transitioning from injury into repair after stroke', *Nat Med*, 14: 497-500.

Lo, E. H., T. Dalkara, and M. A. Moskowitz. 2003. 'Mechanisms, challenges and opportunities in stroke', *Nat Rev Neurosci*, 4: 399-415.

Mattson, M. P., C. Culmsee, and Z. F. Yu. 2000. 'Apoptotic and antiapoptotic mechanisms in stroke', *Cell Tissue Res*, 301: 173-87.

Mehta, S. L., N. Manhas, and R. Raghubir. 2007. 'Molecular targets in cerebral ischemia for developing novel therapeutics', *Brain Res Rev*, 54: 34-66.

Miller, M. C., and K. H. Mayo. 2017. 'Chemokines from a Structural Perspective', *Int J Mol Sci*, 18.

Miron, V. E., A. Boyd, J. W. Zhao, T. J. Yuen, J. M. Ruckh, J. L. Shadrach, P. van Wijngaarden, A. J. Wagers, A. Williams, R. J. M. Franklin, and C. Ffrench-Constant. 2013. 'M2 microglia and macrophages drive oligodendrocyte differentiation during CNS remyelination', *Nat Neurosci*, 16: 1211-18.

Nakka, V. P., A. Gusain, S. L. Mehta, and R. Raghubir. 2008. 'Molecular mechanisms of apoptosis in cerebral ischemia: multiple neuroprotective opportunities', *Mol Neurobiol*, 37: 7-38.

National Institute of Neurological, Disorders, and P. A. Stroke Study Group Stroke rt. 1995. 'Tissue plasminogen activator for acute ischemic stroke', *N Engl J Med*, 333: 1581-7.

Newton, K., A. Strasser, N. Kayagaki, and V. M. Dixit. 2024. 'Cell death', *Cell*, 187: 235-56.

Nicholson, D. W., and N. A. Thornberry. 1997. 'Caspases: killer proteases', *Trends Biochem Sci*, 22: 299-306.

Nijjar, J. S., K. Abbott-Banner, Y. Alvarez, N. Aston, D. Bass, J. H. Bentley, J. Ellis, C. Ellson, E. C. Emery, M. Feeney, D. Fernando, D. Inman, R. Kaur, L. K. Modis, S. Munoz Vicente, C. Muya, K. Nistala, E. Panoilia, R. Ray, S. Siederer, J. E. Smith, L. Weir, and N. Wisniacki. 2025. 'Efficacy, safety and tolerability of GSK3858279, an anti-CCL17 monoclonal antibody and analgesic, in healthy volunteers and patients with knee osteoarthritis pain: a phase I, randomised, double-blind, placebo-controlled, proof-of-mechanism and proof-of-concept study', *Ann Rheum Dis*, 84: 856-65.

Onteniente, B., C. Couriaud, J. Braudeau, A. Benchoua, and C. Guegan. 2003. 'The mechanisms of cell death in focal cerebral ischemia highlight neuroprotective perspectives by anti-caspase therapy', *Biochem Pharmacol*, 66: 1643-9.

Orihuela, R., C. A. McPherson, and G. J. Harry. 2016. 'Microglial M1/M2 polarization and metabolic states', *Br J Pharmacol*, 173: 649-65.

Pan, Y., W. Xin, W. Wei, L. Tatenhorst, I. Graf, A. Popa-Wagner, S. T. Gerner, S. E. Huber, E. Kilic, D. M. Hermann, M. Bahr, H. B. Huttner, and T. R. Doeppner. 2024. 'Knockdown of NEAT1 prevents post-stroke lipid droplet agglomeration in microglia by regulating autophagy', *Cell Mol Life Sci*, 81: 30.

Plociennikowska, A., A. Hromada-Judycka, K. Borzecka, and K. Kwiatkowska. 2015. 'Co-operation of TLR4 and raft proteins in LPS-induced pro-inflammatory signaling', *Cell Mol Life Sci*, 72: 557-81.

Puyal, J., V. Ginet, and P. G. Clarke. 2013. 'Multiple interacting cell death mechanisms in the mediation of excitotoxicity and ischemic brain damage: a challenge for neuroprotection', *Prog Neurobiol*, 105: 24-48.

Radak, D., N. Katsiki, I. Resanovic, A. Jovanovic, E. Sudar-Milovanovic, S. Zafirovic, S. A. Mousad, and E. R. Isenovic. 2017. 'Apoptosis and Acute Brain Ischemia in Ischemic Stroke', *Curr Vasc Pharmacol*, 15: 115-22.

Rayasam, A., M. Hsu, J. A. Kijak, L. Kissel, G. Hernandez, M. Sandor, and Z. Fabry. 2018. 'Immune responses in stroke: how the immune system contributes to damage and healing after stroke and how this knowledge could be translated to better cures?', *Immunology*, 154: 363-76.

Riches, D. W., E. D. Chan, and B. W. Winston. 1996. 'TNF-alpha-induced regulation and signalling in macrophages', *Immunobiology*, 195: 477-90.

Riedl, S. J., and Y. Shi. 2004. 'Molecular mechanisms of caspase regulation during apoptosis', *Nat Rev Mol Cell Biol*, 5: 897-907.

Riezu-Boj, J. I., E. Larrea, R. Aldabe, L. Guembe, N. Casares, E. Galeano, I. Echeverria, P. Sarobe, I. Herrero, B. Sangro, J. Prieto, and J. J. Lasarte. 2011. 'Hepatitis C virus induces the expression of CCL17 and CCL22 chemokines that attract regulatory T cells to the site of infection', *J Hepatol*, 54: 422-31.

Riley, J. S., G. Quarato, C. Cloix, J. Lopez, J. O'Prey, M. Pearson, J. Chapman, H. Sesaki, L. M. Carlin, J. F. Passos, A. P. Wheeler, A. Oberst, K. M. Ryan, and S. W. Tait. 2018. 'Mitochondrial inner membrane permeabilisation enables mtDNA release during apoptosis', *EMBO J*, 37.

Sabogal-Guaqueta, A. M., A. Marmolejo-Garza, V. P. de Padua, B. Eggen, E. Boddeke, and A. M. Dolga. 2020. 'Microglia alterations in neurodegenerative diseases and their modeling with human induced pluripotent stem cell and other platforms', *Prog Neurobiol*, 190: 101805.

Sacco, R. L. 1997. 'Risk factors, outcomes, and stroke subtypes for ischemic stroke', *Neurology*, 49: S39-44.

Sahu, M. P., O. Nikkila, S. Lagas, S. Kolehmainen, and E. Castren. 2019. 'Culturing primary neurons from rat hippocampus and cortex', *Neuronal Signal*, 3: NS20180207.

Sandu, C., E. Gavathiotis, T. Huang, I. Wegorzewska, and M. H. Werner. 2005. 'A mechanism for death receptor discrimination by death adaptors', *J Biol Chem*, 280: 31974-80.

Sandvig, I., I. L. Augestad, A. K. Haberg, and A. Sandvig. 2018. 'Neuroplasticity in stroke recovery. The role of microglia in engaging and modifying synapses and networks', *Eur J Neurosci*, 47: 1414-28.

Saura, J., J. M. Tusell, and J. Serratosa. 2003. 'High-yield isolation of murine microglia by mild trypsinization', *Glia*, 44: 183-9.

Scott, F. L., B. Stec, C. Pop, M. K. Dobaczewska, J. J. Lee, E. Monosov, H. Robinson, G. S. Salvesen, R. Schwarzenbacher, and S. J. Riedl. 2009. 'The Fas-FADD death domain complex structure unravels signalling by receptor clustering', *Nature*, 457: 1019-22.

Sheth, K. N., E. E. Smith, M. V. Grau-Sepulveda, D. Kleindorfer, G. C. Fonarow, and L. H. Schwamm. 2015. 'Drip and ship thrombolytic therapy for acute ischemic stroke: use, temporal trends, and outcomes', *Stroke*, 46: 732-9.

Subedi, L., and B. P. Gaire. 2021. 'Phytochemicals as regulators of microglia/macrophages activation in cerebral ischemia', *Pharmacol Res*, 165: 105419.

Tait, S. W., M. J. Parsons, F. Llambi, L. Bouchier-Hayes, S. Connell, C. Munoz-Pinedo, and D. R. Green. 2010. 'Resistance to caspase-independent cell death requires persistence of intact mitochondria', *Dev Cell*, 18: 802-13.

Tschoe, C., C. D. Bushnell, P. W. Duncan, M. A. Alexander-Miller, and S. Q. Wolfe. 2020. 'Neuroinflammation after Intracerebral Hemorrhage and Potential Therapeutic Targets', *J Stroke*, 22: 29-46.

Tsukahara, T., H. Haniu, T. Uemura, and Y. Matsuda. 2020. 'Therapeutic Potential of Porcine Liver Decomposition Product: New Insights and Perspectives for

Microglia-Mediated Neuroinflammation in Neurodegenerative Diseases', *Biomedicines*, 8.

Uzdensky, A. B. 2018. 'Photothrombotic Stroke as a Model of Ischemic Stroke', *Transl Stroke Res*, 9: 437-51.

van der Worp, H. B., and J. van Gijn. 2007. 'Clinical practice. Acute ischemic stroke', *N Engl J Med*, 357: 572-9.

Varin, A., and S. Gordon. 2009. 'Alternative activation of macrophages: immune function and cellular biology', *Immunobiology*, 214: 630-41.

Vogler, M., Y. Braun, V. M. Smith, M. A. Westhoff, R. S. Pereira, N. M. Pieper, M. Anders, M. Callens, T. Vervliet, M. Abbas, S. Macip, R. Schmid, G. Bultynck, and M. J. Dyer. 2025. 'The BCL2 family: from apoptosis mechanisms to new advances in targeted therapy', *Signal Transduct Target Ther*, 10: 91.

Wajant, H. 2003. 'Death receptors', *Essays Biochem*, 39: 53-71.

Walker, D. G., and L. F. Lue. 2015. 'Immune phenotypes of microglia in human neurodegenerative disease: challenges to detecting microglial polarization in human brains', *Alzheimers Res Ther*, 7: 56.

Wang, G., J. Su, L. Li, J. Feng, L. Shi, W. He, and Y. Liu. 2013. 'Edaravone alleviates hypoxia-acidosis/reoxygenation-induced neuronal injury by activating ERK1/2', *Neurosci Lett*, 543: 72-7.

Wang, J., H. Xing, L. Wan, X. Jiang, C. Wang, and Y. Wu. 2018. 'Treatment targets for M2 microglia polarization in ischemic stroke', *Biomed Pharmacother*, 105: 518-25.

Wang, J., H. Zhuang, X. Yang, Z. Guo, K. Zhou, N. Liu, Y. An, Y. Chen, Z. Zhang, M. Wang, J. Chen, C. Li, and X. Chang. 2024. 'Exploring the Mechanism of Ferroptosis Induction by Sappanone A in Cancer: Insights into the Mitochondrial Dysfunction Mediated by NRF2/xCT/GPX4 Axis', *Int J Biol Sci*, 20: 5145-61.

Wang, Y., J. Huang, Y. Li, and G. Y. Yang. 2012. 'Roles of chemokine CXCL12 and its receptors in ischemic stroke', *Curr Drug Targets*, 13: 166-72.

Wang, Y., S. Wu, Q. Li, H. Sun, and H. Wang. 2023. 'Pharmacological Inhibition of Ferroptosis as a Therapeutic Target for Neurodegenerative Diseases and Strokes', *Adv Sci (Weinh)*, 10: e2300325.

Weber, C., S. Meiler, Y. Doring, M. Koch, M. Drechsler, R. T. Megens, Z. Rowinska, K. Bidzhekov, C. Fecher, E. Ribechini, M. A. van Zandvoort, C. J. Binder, I. Jelinek, M. Hristov, L. Boon, S. Jung, T. Korn, M. B. Lutz, I. Forster, M. Zenke, T. Hieronymus, T. Junt, and A. Zernecke. 2011. 'CCL17-expressing dendritic cells drive atherosclerosis by restraining regulatory T cell homeostasis in mice', *J Clin Invest*, 121: 2898-910.

Whiteley, W., W. L. Chong, A. Sengupta, and P. Sandercock. 2009. 'Blood markers for the prognosis of ischemic stroke: a systematic review', *Stroke*, 40: e380-9.

Wieloch, T., and K. Nikolich. 2006. 'Mechanisms of neural plasticity following brain injury', *Curr Opin Neurobiol*, 16: 258-64.

Woolf, Z., T. J. Stevenson, K. Lee, Y. Jung, T. I. H. Park, M. A. Curtis, J. M. Montgomery, and M. Dragunow. 2021. 'Isolation of adult mouse microglia using their in vitro adherent properties', *STAR Protoc*, 2: 100518.

Xiao, P., H. Huang, H. Zhao, R. Liu, Z. Sun, Y. Liu, N. Chen, and Z. Zhang. 2024. 'Edaravone dexborneol protects against cerebral ischemia/reperfusion-induced blood-brain barrier damage by inhibiting ferroptosis via activation of nrf-2/HO-1/GPX4 signaling', *Free Radic Biol Med*, 217: 116-25.

Xue, Y., D. Nie, L. J. Wang, H. C. Qiu, L. Ma, M. X. Dong, W. J. Tu, and J. Zhao. 2021. 'Microglial Polarization: Novel Therapeutic Strategy against Ischemic Stroke', *Aging Dis*, 12: 466-79.

Yao, H., R. Takasawa, K. Fukuda, D. Shiokawa, F. Sadanaga-Akiyoshi, S. Ibayashi, S. Tanuma, and H. Uchimura. 2001. 'DNA fragmentation in ischemic core and penumbra in focal cerebral ischemia in rats', *Brain Res Mol Brain Res*, 91: 112-8.

Ye, Y., T. Jin, X. Zhang, Z. Zeng, B. Ye, J. Wang, Y. Zhong, X. Xiong, and L. Gu. 2019. 'Meisoindigo Protects Against Focal Cerebral Ischemia-Reperfusion Injury by Inhibiting NLRP3 Inflammasome Activation and Regulating

Microglia/Macrophage Polarization via TLR4/NF-kappaB Signaling Pathway', *Front Cell Neurosci*, 13: 553.

Yosefzon, Y., D. Soteriou, A. Feldman, L. Kostic, E. Koren, S. Brown, R. Ankawa, E. Sedov, F. Glaser, and Y. Fuchs. 2018. 'Caspase-3 Regulates YAP-Dependent Cell Proliferation and Organ Size', *Mol Cell*, 70: 573-87 e4.

Zhang, A., Y. Liu, H. Xu, Z. Zhang, X. Wang, L. Yuan, C. Lenahan, C. Zhang, J. Jiang, C. Fang, Y. Fang, J. Zhang, and S. Chen. 2022. 'CCL17 exerts neuroprotection through activation of CCR4/mTORC2 axis in microglia after subarachnoid haemorrhage in rats', *Stroke Vasc Neurol*, 8: 4-16.

Zhang, R., M. Chopp, and Z. G. Zhang. 2013. 'Oligodendrogenesis after cerebral ischemia', *Front Cell Neurosci*, 7: 201.

Zhao, H., M. A. Yenari, D. Cheng, R. M. Sapolsky, and G. K. Steinberg. 2003. 'Bcl-2 overexpression protects against neuron loss within the ischemic margin following experimental stroke and inhibits cytochrome c translocation and caspase-3 activity', *J Neurochem*, 85: 1026-36.

Zi, Y., X. Wang, Y. Zi, H. Yu, Y. Lan, Y. Fan, C. Ren, K. Liao, and H. Chen. 2023. 'Cigarette smoke induces the ROS accumulation and iNOS activation through deactivation of Nrf-2/SIRT3 axis to mediate the human bronchial epithelium ferroptosis', *Free Radic Biol Med*, 200: 73-86.

Ehrenwörtliche Erklärung

„Hiermit erkläre ich, dass ich die vorliegende Arbeit selbständig und ohne unzulässige Hilfe oder Benutzung anderer als der angegebenen Hilfsmittel angefertigt habe. Alle Textstellen, die wörtlich oder sinngemäß aus veröffentlichten oder nichtveröffentlichten Schriften entnommen sind, und alle Angaben, die auf mündlichen Auskünften beruhen, sind als solche kenntlich gemacht. Bei den von mir durchgeführten und in der Dissertation erwähnten Untersuchungen habe ich die Grundsätze guter wissenschaftlicher Praxis, wie sie in der „Satzung der Justus-Liebig-Universität Gießen zur Sicherung guter wissenschaftlicher Praxis“ niedergelegt sind, eingehalten sowie ethische, datenschutzrechtliche und tierschutzrechtliche Grundsätze befolgt. Ich versichere, dass Dritte von mir weder unmittelbar noch mittelbar geldwerte Leistungen für Arbeiten erhalten haben, die im Zusammenhang mit dem Inhalt der vorgelegten Dissertation stehen, und dass die vorgelegte Arbeit weder im Inland noch im Ausland in gleicher oder ähnlicher Form einer anderen Prüfungsbehörde zum Zweck einer Promotion oder eines anderen Prüfungsverfahrens vorgelegt wurde. Alles aus anderen Quellen und von anderen Personen übernommene Material, das in der Arbeit verwendet wurde oder auf das direkt Bezug genommen wird, wurde als solches kenntlich gemacht. Insbesondere wurden alle Personen genannt, die direkt und indirekt an der Entstehung der vorliegenden Arbeit beteiligt waren. Mit der Überprüfung meiner Arbeit durch eine Plagiatserkennungssoftware bzw. ein internetbasiertes Softwareprogramm erkläre ich mich einverstanden.“

_____ _____

Ort/Datum Unterschrift

ACKNOWLEDGEMENT

At the moment of graduation, looking back on the past fills me with deep emotion.

I wish to extend my heartfelt appreciation to my supervisor, Professor Thorsten Roland Döppner. He provided every possible condition for many of my ideas, greatly helping me realize my goals smoothly and serving as a strong pillar of support.

I am deeply thankful to the postdoc, Dr. Sabine Huber, and Dr. Samir Vaid, who offered invaluable advice and always spoke candidly and wholeheartedly.

At the same time, I'm incredibly grateful to my peers and friends who have accompanied and encouraged me in both my studies and my life.

I would like to sincerely thank my grandmother and parents for their unwavering support throughout my life.